

國立臺灣大學電機資訊學院電機工程學系

碩士論文

Department of Electrical Engineering

College of Electrical Engineering and Computer Science

National Taiwan University

Master Thesis

多階態開路電壓和短路電流感測金氧半耦合元件及誘

導式軟性崩潰操作技術

Multi-State Open-Circuit Voltage and Short-Circuit  
Current Sensing in MIS Coupling Devices and Induced  
Soft Breakdown Operation Technology

陳舜啓

Shun-Chi Chen

指導教授：胡振國 博士

Advisor: Jenn-Gwo Hwu, Ph.D.

中華民國 112 年 6 月

June 2023

國立臺灣大學碩士學位論文  
口試委員會審定書

MASTER'S THESIS ACCEPTANCE CERTIFICATE  
NATIONAL TAIWAN UNIVERSITY

多階態開路電壓和短路電流感測金氧半耦合元件及誘導式軟  
性崩潰操作技術

Multi-State Open-Circuit Voltage and Short-Circuit Current  
Sensing in MIS Coupling Devices and Induced Soft Breakdown  
Operation Technology

本論文係陳舜啓(R10943062)在國立臺灣大學電子工程學研究所完成之碩士學位論文，於民國 112 年 6 月 9 日承下列考試委員審查通過及口試及格，特此證明。

The undersigned, appointed by the Department / Institute of Electronics Engineering National Taiwan University On 9(date) 6(month) 2023(year) have examined a Master's thesis entitled above presented by Shun-Chi Chen (R10943062) candidate and hereby certify that it is worthy of acceptance.

口試委員 Oral examination committee:

胡振國  
(指導教授 Advisor)

吳幼麟

胡隱合

系主任/所長 Director: \_\_\_\_\_

江介宏

## 誌謝

在碩士求學階段受到很多貴人幫助，首先謝謝我的指導老師胡振國教授，在這兩年的每周會議老師都很盡心盡力的和我一起討論研究內容，也在討論過程中以及老師的課堂中感受到老師非常札實的半導體物理知識，因此老師最常叮囑的就是基本功要練好，因為做研究就是必須一步一步來，馬步蹲穩了才能把研究做好。也非常感謝兩位口試委員胡璧合教授、吳幼麟教授在口試時給予了許多寶貴的建議和指導。

也謝謝實驗室的各位，謝謝林冠文、陳冠竹學長打理實驗大小事，以及黃崧璋學長總是能提供我在研究上的建議和方向，不論是製程、量測、模擬，你都提供了很多的建議和協助；謝謝我同屆的同學沈祐德、林郁芹、高綺憶、林軒毅，能和你們一起修課、互相討論研究內容，都是碩士生涯很重要的回憶；也謝謝學弟妹們承接實驗室的大小事務，也祝福你們未來都順利。

最後感謝我的父母和家人們，謝謝你們養育我、關心我，讓我能順利地完成學業，雖然在過程中遇到了很多困難，但也因為有你們我才能堅持地走到最後，也謝謝我的女朋友，陪我度過了許多在台大校園的日子，也同時分擔了我的壓力和煩惱，讓我的碩士求學之路不孤單。最後獻給在天上的父親，我成功完成學業了，雖然您沒能陪我走到畢業這天，但你的心永遠與我同在。



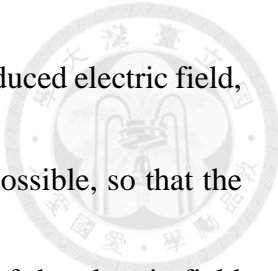
## 摘要

本篇論文主要探討金氧半穿隧元件的耦合效應及開路電壓和短路電流感測的多階態特性，元件的電極結構為四個正方形圍繞著一個長方形。在本論文第二章中，金氧半元件因有超薄氧化層的設計，因此可以有極小的飽和電流，並且透過電流-電壓量測後可發現有耦合效應。當外環施加偏壓時，其中心可感應到開路電壓及短路電流，並且隨著外環的數量不同，中心所感應的開路電壓和短路電流也有明顯區別，因此可作為多階態展現的金氧半元件。在本論文第三章中，為了較相容現今的技術節點，因此利用厚薄氧化層的製程將元件微縮，並且採用先生長厚氧化層再生長薄氧化層的方式，厚薄氧化層的元件會因為厚區不斷提供少數載子至薄區，因此電流無法達到飽和也無耦合效應。本研究提出了特別的引導式軟性崩潰操作，可以使氧化層局部薄化，將元件的特性改變，使得電流進入飽和並且開路電壓有耦合效應，元件也能展現出多階態特性。特別的軟性崩潰方法是利用感應電場的分布不均，將外環和中心的氧化層局部薄化點盡可能的靠近，因此能使耦合效應增強。為了能驗證電場和電子濃度的分布，使用了 SILVACO TCAD 軟體進行電場和電子濃度的模擬，結果也和所提出的想法相符合。因此，不論是超薄氧化層或是厚薄氧化層的金氧半穿隧元件，都具有作為多階態特性元件的潛力。

## Abstract



In this thesis, the coupling effect of the metal insulator semiconductor tunneling diodes (MIS TD) and the multi-state characteristics of open-circuit voltage and short-circuit current sensing of the device have been investigated. The electrode pattern of the device is four squares surrounding a rectangle. In **Chapter 2**, due to the design of the ultra-thin oxide layer, the device has extremely low saturation current. The coupling effect was found through the current-voltage measurement. Applying a bias voltage to the outer rings, the open-circuit voltage and the short-circuit current were sensed in the center. The magnitude of sensed open-circuit voltage and sensed short-circuit current are also significantly different with different number of outer rings, so it can be used as a multilevel device. In **Chapter 3**, in order to be compatible with current technology nodes, the device is scaled by the high-low oxide process. The method of growing thick oxide first and then thin oxide is used. Because the thick oxide region will provide extra minority carriers to the thin oxide region, there would be no saturation current and no coupling effect of the device. Therefore, a special method of induced soft breakdown operation was proposed, which can create the oxide local thinning (OLT) and change the characteristics of the device. The current is saturated and the open-circuit voltage exhibits coupling effect. Hence, the device can also exhibit multi-level characteristic. The special



soft breakdown operation is based on the uneven distribution of the induced electric field, and to make OLT spot of the outer rings and the center as close as possible, so that the coupling effect can be enhanced. In order to verify the distribution of the electric field and the electron concentration, SILVACO TCAD software is used to simulate the electric field and the electron concentration. The result is consistent with the proposed method. Therefore, both of MIS tunneling diodes with ultra-thin oxide and high-low oxide have the potential to be used as multi-state characteristic devices.



# Contents



摘要.....	I
<b>Abstract</b> .....	II
<b>Contents</b> .....	IV
<b>Figure Captions</b> .....	VII
<b>Chapter 1 Introduction</b> .....	1
1-1 Thesis Organization.....	2
1-2 I-V Characteristics of MIS(p) Tunnel Diodes.....	2
1-2-1 Mechanism of Hole Current Saturation.....	2
1-2-2 Effect of Oxide Thickness.....	3
1-2-3 Effect of Additional Minority Carriers Supply.....	4
1-3 OLT (Oxide Local Thinning).....	5
1-4 TCAD Simulation.....	6
1-5 Summary.....	6
<b>Chapter 2 Multi-State Displayed by Open-Circuit Voltage and Short-Circuit Current of Coupling MIS TD</b> .....	11
2-1 Introduction.....	12
2-2 Experimental Procedure.....	12



2-3 Results and Discussions.....13

    2-3-1 I-V Characteristics in Planar Structure Operation.....13

    2-3-2 Open-Circuit Operation of Coupling Voltage.....13

    2-3-3 Short-Circuit Operation of Coupling Current.....14

    2-3-4 Multi-State Voltage/Current by Different Structure.....15

2-4 Summary.....16

### **Chapter 3 Coupling Effect of High-Low Structure MIS TD**

#### **Enhanced by Novel Soft Breakdown Operation.....33**

3-1 Introduction.....34

3-2 Experimental Procedure.....34

3-3 Results and Discussions.....36

    3-3-1 I-V Characteristics in Planar and High-Low Structure.....36

    3-3-2 Soft Breakdown Mechanism in High-Low Device.....37

    3-3-3 Ring Soft Breakdown Induced by Center with Negative bias.....39


    3-3-4 Electric Field and Electron Concentration in TCAD

        Simulation.....41

3-4 Summary.....43

### **Chapter 4 Conclusion and Future Work.....61**





4-1 Conclusion.....	62
4-2 Future Work.....	63
4-2-1 More Input and Output Combinations for Multi-State Characteristic.....	63
4-2-2 Process for High-Low Structure.....	63
4-2-3 The Pattern of Electrode.....	64
<b>References.....</b>	<b>66</b>

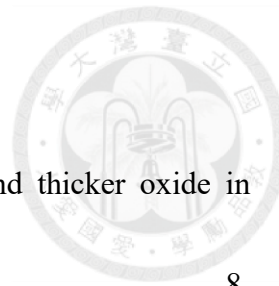


## Figure Captions

<b>Fig. 1-1.</b> The energy band diagrams of MIS TDs with thinner and thicker oxide in saturation region [2].....	8
<b>Fig. 1-2.</b> I-V characteristics of MIS(p) TD with various oxide thickness [2].....	8
<b>Fig. 1-3.</b> I-V characteristics of MIS(p) TD with different oxide thickness in dark and under light conditions [4].....	9
<b>Fig. 1-4.</b> The energy band diagrams of MIS TDs with less and more electrons supply in saturation region [2].....	9
<b>Fig. 1-5.</b> Schematics of the OLT will at edge of the MIS(p) TD after positive bias [6].....	10
<b>Fig. 2-1.</b> Schematic top view of the 4 rings MIS TD device.....	17
<b>Fig. 2-2.</b> Schematic top view of the 4 rings MIS TD device with circular pad.....	17
<b>Fig. 2-3.</b> Schematic top view of the center MIS TD device.....	18
<b>Fig. 2-4.</b> I-V curves of the center MIS TD.....	19
<b>Fig. 2-5.</b> C-V curves of the center MIS TD.....	19
<b>Fig. 2-6.</b> 3D schematic top view of (a) the 4 rings (n2f2), (b) the 3 rings (n2f1) and the 1 ring (f1), (c) the 3 rings (n1f2) and the 1 ring (n1), (d) the 2 rings (n2) and (f2), and (e) the 2 rings (n1f1) MIS TD devices. n means near and f means farther.....	21
<b>Fig. 2-7.</b> Schematic of open-circuit voltage operation.....	22

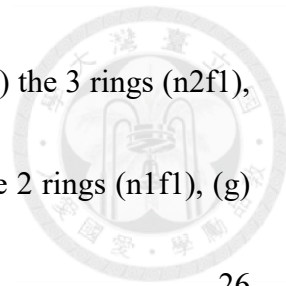


**Fig. 2-8.**  $I_{ring}$  &  $V_{center}$  versus  $V_{ring}$  curves of (a) the 4 rings (n2f2), (b) the 3 rings (n2f1), (c) the 3 rings (n1f2), (d) the 2 rings (n2), (e) the 2 rings (f2), (f) the 2 rings (n1f1), (g) the 1 ring (n1), and (h) the 1 ring (f1) MIS TD devices.....26

**Fig. 2-9.** Schematic of short-circuit current operation.....27

**Fig. 2-10.**  $I_{ring}$  &  $I_{sc(center)}$  versus  $V_{ring}$  curves of (a) the 4 rings (n2f2), (b) the 3 rings (n2f1), (c) the 3 rings (n1f2), (d) the 2 rings (n2), (e) the 2 rings (f2), (f) the 2 rings (n1f1), (g) the 1 ring (n1), and (h) the 1 ring (f1) MIS TD devices.....31

**Fig. 2-11.** Error bar chart of coupling open-circuit voltages with different inputs.....32

**Fig. 2-12.** Error bar chart of coupling short-circuit currents with different devices.....32

**Fig. 3-1.** Schematic top view of the high-low center MIS TD device.....44

**Fig. 3-2.** Schematic top view of the 4 rings high-low MIS TD device with circular pad...44

**Fig. 3-3.** I-V curves of the thick oxide center MIS TD.....45

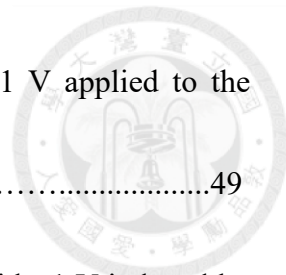
**Fig. 3-4.** 3D Schematic top view of the high-low center MIS TD device.....46

**Fig. 3-5.** I-V curves of the high-low oxide center MIS TD.....46

**Fig. 3-6.** I-V curves of the planar and high-low center MIS TD.....47

**Fig. 3-7.** I-V curves of (a) the center MIS TD with soft breakdown operation and (b) the 4 rings MIS TD with proceeded soft breakdown operation.....48

**Fig. 3-8.** I-V curves of (a) the center MIS TD with soft breakdown operation and (b) the



4 rings MIS TD with proceeded soft breakdown operation with -1 V applied to the center.....49

**Fig. 3-9.** Coupled voltage of  $V_{ring}$  versus time (a) without and (b) with -1 V induced by center during ring soft breakdown operation.....50

**Fig. 3-10.**  $I_{center}$  &  $V_{ring}$  versus  $V_{center}$  curves of (a) the 4 rings, (b) the 3 rings, (c) the 2 rings, (d) the 1 ring MIS TD.....52

**Fig. 3-11.** Schematic of the TCAD simulation device for planar oxide.....53

**Fig. 3-12.** (a) Electric field with  $V_{Ring1} = V_{Ring2} = 0$  V,  $V_c = 5$  V for planar oxide. (b) Zoom in electric field of (a).....54

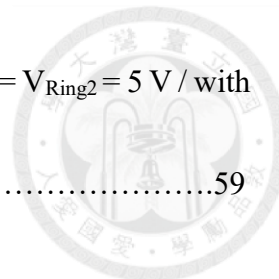
**Fig. 3-13.** Schematic of the TCAD simulation device with OLT at the edge of center oxide.....55

**Fig. 3-14.** Electric field distributions with (a)  $V_{Ring1} = V_{Ring2} = 3$  V /  $V_c = -1$  V, (b) with  $V_{Ring1} = V_{Ring2} = 4$  V /  $V_c = -1$  V, and (c) with  $V_{Ring1} = V_{Ring2} = 5$  V /  $V_c = -1$  V, for device with OLT at the edge of center oxide.....56

**Fig. 3-15.** Electron concentration distribution with  $V_{Ring1} = V_{Ring2} = 3$  V /  $V_c = -1$  V of the device with OLT at the edge of center oxide.....57

**Fig. 3-16.** (a) Electric field and (b) Electron concentration with  $V_{Ring1} = V_{Ring2} = 5$  V for center floating condition. The center set voltage is  $V_{set@I=0} = V_{oc(coupled)} = 0.425$  V.....58

**Fig. 3-17.** (a) Electric field and (b) Electron concentration with  $V_{\text{Ring1}} = V_{\text{Ring2}} = 5 \text{ V}$  / with center bias voltage of  $V_c = 3\text{V}$ .....59





# **Chapter 1**

## **Introduction**

### **1-1 Thesis Organization**

### **1-2 I-V Characteristics of MIS(p) Tunnel Diodes**

#### **1-2-1 Mechanism of Hole Current Saturation**

#### **1-2-2 Effect of Oxide Thickness**

#### **1-2-3 Effect of Additional Minority Carriers Supply**

### **1-3 OLT (Oxide Local Thinning)**

### **1-4 TCAD Simulation**

### **1-5 Summary**





## 1-1 Thesis Organization

In this thesis, the sensing characteristic of coupling MIS TD were discussed. The low power consumption of MIS TD with multi-state characteristic is of interest. In **Chapter 2**, the MIS TD of planar structures having 4 rings, 3 rings, 2 rings, and 1 ring were proposed. With different inputs of devices, the sensed open-circuit voltage and the sensed short-circuit current of the center can both show multilevel characteristics. In order to reduce the area of the device. **Chapter 3** proposed the structure of high-low oxide. It was noticed that we grew the thick oxide region first and then grew the thin oxide region, and both the center and the ring were located at the thin oxide region. It was found that the thick oxide region will provide extra minority carriers to the thin oxide region, and therefore the high-low structure cannot have a saturation current under the reverse bias. In this work, the operation of soft breakdown with current compliance and the operation of soft breakdown induced by special negative biasing were proposed. It was found that the device can still display the multi-state characteristic. Last but not least, **Chapter 4** is a conclusion of this thesis, and makes some suggestions and improvements for the future work.

## 1-2 I-V Characteristics of MIS(p) Tunnel Diodes

### 1-2-1 Mechanism of Hole Current Saturation

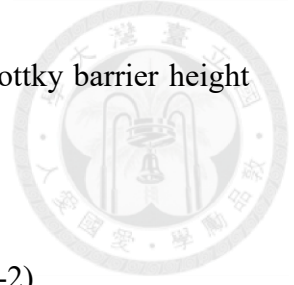
For the device of MIS(p) TD, it was found that the hole current dominates the saturation current in the reverse bias, which can be expressed by eq. (1-1) [1],

$$I_h = A^* A_{eff} P_t T^2 e^{\frac{-q\phi_h^*}{kT}}, \quad (1-1)$$

where  $I_h$  is the hole current,  $A^*$  is the effective Richardson constant,  $A_{eff}$  is the effective area,  $P_t$  is the tunneling probability,  $T$  is the temperature of the device,  $\phi_h^*$  is the effective Schottky barrier height,  $q$  is the electron charge, and  $k$  is the Boltzmann constant. When reverse bias is large enough to exceed a certain bias, the electric field in the oxide layer is strong, and the tunneling rate will be too large so that inversion charges cannot be accumulated at the interface of  $\text{SiO}_2/\text{Si}$ . This is called deep depletion that the oxide voltage will be fixed and any additional voltage will drop on silicon substrate. This is the reason why the current will be saturated in the reverse bias.

### **1-2-2 Effect of Oxide Thickness**

The accumulation current operating under forward bias will vary with the thickness of the oxide layer. Because the electron flow dominates under forward bias, the accumulation current is larger for the thinner oxide layer due to the higher electron tunneling rate. Therefore, the accumulation current of thicker oxide layer is small. Conversely, the saturation current of operating in reverse bias, the saturation current is larger in the thicker oxide layer and smaller in the thinner oxide layer [2]. The reason for



this phenomenon is due to Schottky barrier height modulation. Schottky barrier height can be expressed by the following eq. (1-2) [1],

$$\varphi_h^* = \chi_s - \Phi_m + \frac{E_g}{q} - V_{ox} \quad , \quad (1-2)$$

where  $\chi_s$  is electron affinity of the semiconductor,  $\Phi_m$  is the work function of the metal,  $E_g$  is the energy band gap of the semiconductor,  $V_{ox}$  is the fixed oxide voltage,  $q$  is the electron charge, respectively. Fig. 1-1 show the energy band diagrams of MIS TDs with thinner and thicker oxide in saturation region [2]. When the same voltage is applied on the device, the thinner oxide layer has a higher tunneling rate and a smaller voltage dropped on the thin oxide layer. Therefore, it was resulting in a larger effective Schottky barrier height  $\varphi_{h1}^*$  and a smaller hole current  $I_{h1}$  will be obtained; Conversely, the device of the thicker oxide layer has a larger voltage, resulting in smaller  $\varphi_{h2}^*$  and larger  $I_{h2}$ . The I-V curves of MIS(p) TD with different oxide thickness was shown in Fig. 1-2 [2].

### 1-2-3 Effect of Additional Minority Carriers Supply

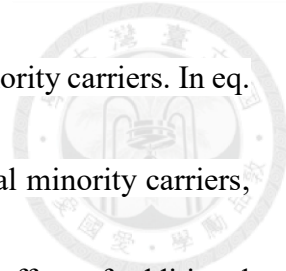
The Schottky barrier height is related to the supplementation of minority carriers, which can be supplied by photo-generation [3] or the neighboring region of thick oxide.

It can be expressed by the following equation [2].

$$\varphi_h^* = \varphi_{h0} - \Delta\varphi_h \quad (1-3)$$

$$\Delta\varphi_h = Bq|F|d_{ox} \quad (1-4)$$

In eq. (1-3),  $\varphi_h^*$  is the effective Schottky barrier height,  $\Delta\varphi_h$  is the reduction of the



Schottky barrier height,  $\phi_{h0}$  is the Schottky barrier height without minority carriers. In eq. (1-4),  $B$  is a constant,  $q$  is the electron charge,  $F$  represents the lateral minority carriers,  $d_{ox}$  is the oxide thickness. Fig. 1-3 [4] and Fig. 1-4 [2] shows the effect of additional minority carriers supply. The more minority carriers accumulate at the Si/SiO<sub>2</sub> interface will cause a larger  $V_{ox}$  and a smaller  $\phi_h^*$  will be obtained [2]. Thus, resulting in a large saturation current. According to the above reasons, minority carriers will affect the effective Schottky barrier height under the reverse bias, which is also the key to determining the saturation current. However, there is no shortage of minority carriers in the accumulation region under the forward bias, so there is no such effect.

### **1-3 OLT (Oxide Local Thinning)**

When the device was applied with a stress or a sweeping voltage, the I-V characteristics of the device will be different. For example, the current will not be saturated under the reverse bias of the high-low oxide structure. Sweeping bias voltage can be used for the operation of soft breakdown, and the current of the device after soft breakdown can also be saturated. The mechanism of soft breakdown is that a local bulk trap in oxide will cause the tunneling current to rise [5], and the damaged region can be regarded as oxide local thinning (OLT) as shown in Fig. 1-4 [6] [7]. OLT usually occurs around the edge of the device because of the fringing field effect [8] [9] [10]. The

saturation current usually tunneled by the edge of the device because of the fringing field effect. After the OLT formed on the edge of the device, a lot of minority carriers were more likely to pass through the oxide local thinning layer [6], and caused the current to be saturated easier.

## 1-4 TCAD Simulation

In order to verify the experimental data and prove the electric field distribution of soft breakdown, software simulation of SILVACO TCAD including S.EDA tools like Deck Build and TonyPlot were used 2D MIS structure was considered in the simulation. The device is mainly composed of three adjacent metals for aluminum as the electrode, ultra-thin oxide layer as the insulator, and p type Si as substrate. The metal work function of aluminum is 4.1 eV and p type substrate doping is  $1 \times 10^{16} \text{ cm}^{-3}$ . In addition, the segmentation of the mesh is also very important. If the mesh is meticulous, the device characteristic can be analyzed more precisely, but it may also cause the process of calculation not to converge in the simulation, and the simulation result will fail. Hence, the mesh must be finely set at the boundary of the electrode and OLT, and the other mesh can be broader to achieve the balance of mesh division.

## 1-5 Summary

In this chapter, the thesis organization including the characteristics of MIS(p) TD, I-

V curves, mechanism of the hole saturation current, the effect of oxide thickness of forward/reverse bias, Schottky barrier height modulation, additional minority carriers supply, OLT caused by soft breakdown, TCAD simulation were introduced. After having a knowledge of the basic properties of MIS TD, device sensing was explored in the next chapters.



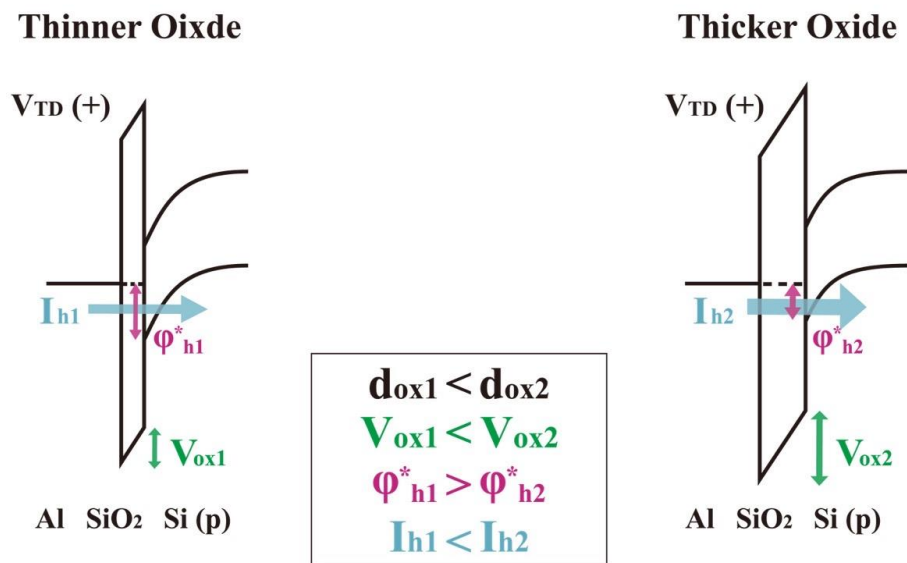


Fig. 1-1 The energy band diagrams of MIS TDs with thinner and thicker oxide in saturation region [2].

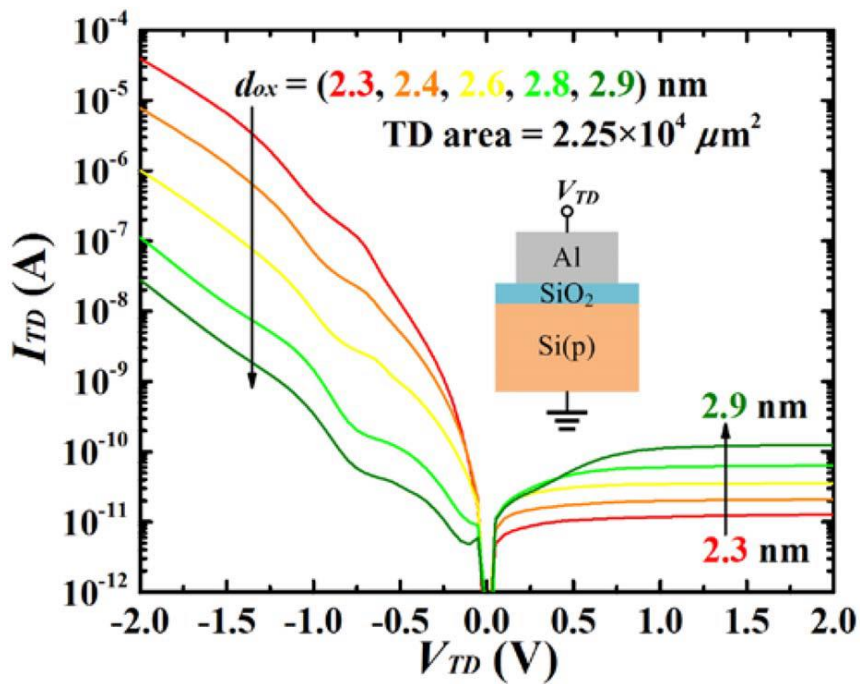


Fig. 1-2 I-V characteristics of MIS(p) TD with various oxide thickness [2].

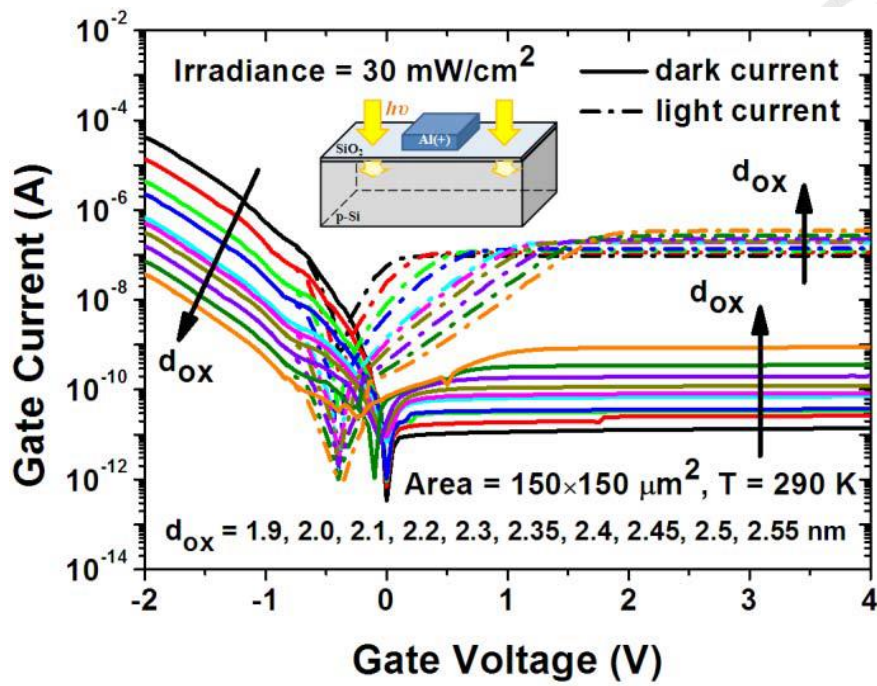


Fig. 1-3 I-V characteristics of MIS(p) TD with different oxide thickness in dark and under light conditions [4].

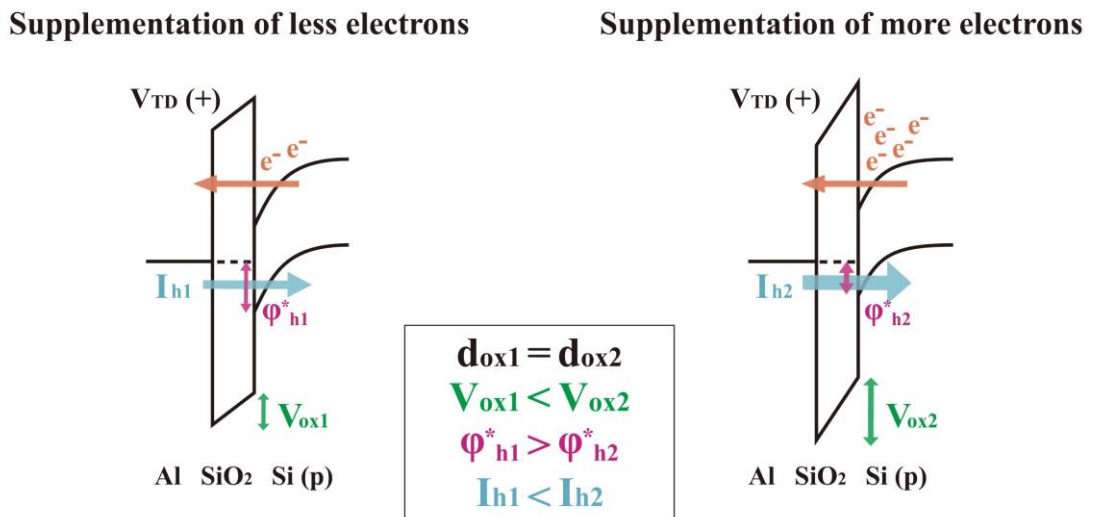


Fig. 1-4 The energy band diagrams of MIS TDs with less and more electrons supply in saturation region [2].

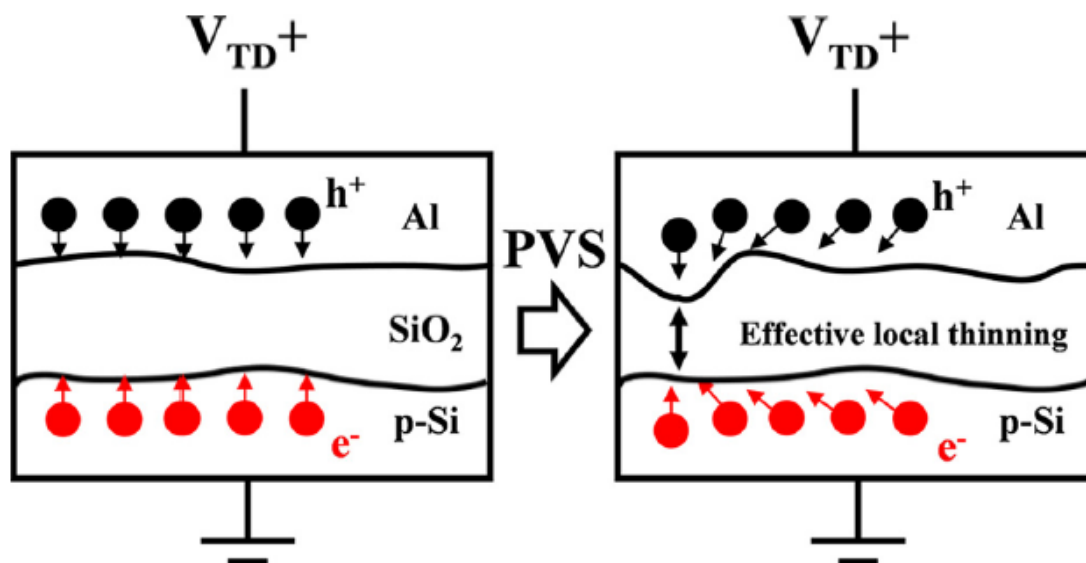


Fig. 1-5 Schematics of the OLT will at edge of the MIS(p) TD after positive bias [6].



## **Chapter 2**

# **Multi-State Displayed by Open-Circuit Voltage and Short-Circuit Current of Coupling MIS TD**

### **2-1 Introduction**

### **2-2 Experimental Procedure**

### **2-3 Results and Discussions**

#### **2-3-1 I-V Characteristics in Planar Structure Operation**

#### **2-3-2 Open-Circuit Operation of Coupling Voltage**

#### **2-3-3 Short-Circuit Operation of Coupling Current**

#### **2-3-4 Multi-State Voltage/Current by Different Structure**

### **2-4 Summary**

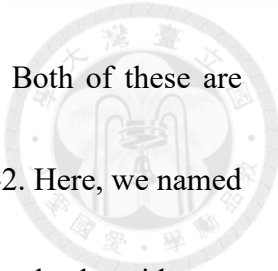


## 2-1 Introduction

In **Chapter 1**, we have discussed the characteristics of MIS TD. When operating in inversion region, the current will be saturated and the value is extremely low, which can achieve the effect of low power consumption. In this chapter, MIS TD with different structures will be explained. They are 4 outer rings, 3 outer rings, 2 outer rings and 1 outer ring. Because the area of the outer ring and the central region are small, it must be connected to a pad with a large area that can be available for measurement. The open-circuit voltage and short-circuit current of the central region are considered in this work. The phenomenon of multi-state characteristics are discussed.

## 2-2 Experimental Procedure

A boron-doped 1-10  $\Omega$ -cm (100) p-type silicon wafer was used as the substrate. At first, we use standard Radio Corporation of America (RCA) to remove impurity particles, native oxide and organic impurities. A thin oxide layer was grown by anodic oxidation in D.I. water and the oxide layer thickness was about 2.3 nm [11]. Rapid thermal process at 950°C for 15 seconds was used for post-oxidation annealing. The 200 nm Al film was deposited on the oxide layer by thermal evaporation. To design the pattern on device, we defined the pattern by photolithography and wet etching. The top view of the device was shown in Fig. 2-1. The central region is a rectangle and the size is 50  $\mu\text{m}$   $\times$  20  $\mu\text{m}$ . The



outer region are four squares and the size are all  $15\ \mu\text{m} \times 15\ \mu\text{m}$ . Both of these are connected to a circular pad with a radius of  $85\ \mu\text{m}$  as shown in Fig. 2-2. Here, we named the central region as center and the outer region as ring. Finally, the back oxide was removed by buffered oxide etch (BOE). A 250 nm Al film was evaporated on the back side as back contact. The electrical characteristics and analysis were measured by Agilent B1500A in dark environment.

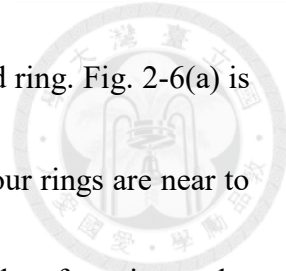
## **2-3 Results and Discussion**

### **2-3-1 I-V Characteristics in Planar Structure Operation**

First, we observed the I-V curves of the center. Fig. 2-3 is the top view of the center device. In Fig. 2-4, it can be clearly seen that when the device operated in negative bias, which is under forward bias (accumulation) region, the current value is very large; and when operated in positive bias, which is under reverse bias (inversion) region, the current value is much lower and tends to be saturated. This is a typical I-V characteristics of the ultra-thin oxide layer of MIS TD. The effect of low power consumption can be achieved by operating the device in the reverse bias region. C-V curves of the center region was shown in Fig. 2-5. The accumulation capacitance drops to negative value because the oxide layer is too thin to cause leakage of current.

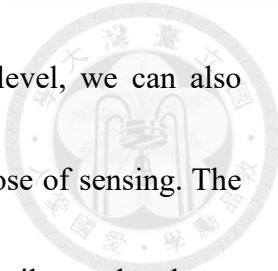
### **2-3-2 Open-Circuit Operation of Coupling Voltage**





Next, we will discuss the coupling effect between the center and ring. Fig. 2-6(a) is a 3D view of the device with four rings and center, and two of the four rings are near to the center, and the other two are farther away from the center. Therefore, it can be subdivided into n (near to the center) and f (farther to the center). The 4 rings can be regarded as 4 inputs, abbreviated as n2f2. Fig. 2-6(b) and Fig. 2-6(c) showed 3 rings and 1 ring, which can be subdivided into n2f1, f1, n1f2, and n1. Fig. 2-6(d), and Fig. 2-6(e) showed 2 rings, which can be divided into n2, f2, and n1f1. Ring can be used as an input and center is a sensor. Fig. 2-7 shows the measurement procedure of applying a bias voltage of -1V~5V at ring, and then read the open-circuit voltage sensed by center. Because the distance between ring and center is only 5  $\mu\text{m}$ , there will be a coupling effect between the two, which will cause the induced open-circuit voltage in the center when the bias voltage of ring was swept to 5V. These devices can be divided into different inputs, and the results obtained are also different. Figs. 2-8(a)~(h) showed the sensed coupling voltage at center  $V_{\text{center}}$  along with  $I_{\text{ring}}$  for 4 inputs (4 rings), 3 inputs (3 rings), 2 inputs (2 rings), and 1 input (1 ring) operations. It is obvious that the more the number of inputs, the larger the open-circuit voltage sensed at center. The multi-state characteristic was observed.

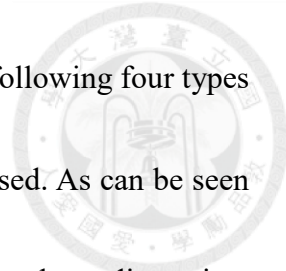
### **2-3-3 Short-Circuit Operation of Coupling Current**



In addition to using the open-circuit voltage to display multilevel, we can also measure the short-circuit current of device to achieve the same purpose of sensing. The schematic diagram is shown in Fig. 2-9. The operation process is similar to the above, and a bias voltage of  $-1\text{ V}\sim 5\text{ V}$  is applied to the ring, but the center needs to be short-circuited and short-circuit current was measured. The short-circuit current is not only related to several inputs, but also related to the distance between the ring and the center's pad. For example, the 3 inputs can be divided into  $n_2f_1$  and  $n_1f_2$ . The short-circuit currents of the two will be different. The  $n_2f_1$  will be slightly larger than  $n_1f_2$  because in this case it will be dominated by  $n$  ( $n_2>n_1$ ). Figs. 2-10(a)~(h) showed the coupling short-circuit currents of different devices. Multilevel characteristics can be determined by the proper choice of device structure.

### **2-3-4 Multistate Voltage/Current by Different Structure**

Fig. 2-11 shows the error bar chart of coupling voltage with different inputs. For the open-circuit voltage, the level of sensed voltage is only related to how many inputs the device owns, and the distance between the ring and the center does not affect its coupling voltage. However, for the measurement of short-circuit current, the distance between the ring and the center will have a significant impact. Generally speaking, the closer the distance of ring to center, the larger the sensed short-circuit current, and the farther away



from the center, the smaller the contribution of the ring. Finally, the following four types of 4 rings ( $n_2f_2$ ), 3 rings ( $n_1f_2$ ), 2 rings ( $f_2$ ) and 1 ring ( $f_1$ ) are focused. As can be seen in Fig. 2-12, multi-state characteristics are also displayed. Based on the above discussion, both the open-circuit voltage and the short-circuit current have coupling effect and exhibit multistate characteristics.

## 2-4 Summary

In this chapter, MIS TD with different novel structures of 4 rings, 3 rings, 2 rings and 1 ring are proposed. By using the MIS TD coupling mechanism and ultra-low saturation current in the inversion region, different numbers of rings can give the multilevel effect. There are two parts to discuss. The first part is to apply a bias voltage of 5V at the ring, and the center of 4 rings, 3 rings, 2 rings and 1 ring can sense different open-circuit voltages; the second part is to apply a bias voltage of 5V at the ring, and the centers of  $n_2f_2$ ,  $n_1f_2$ ,  $f_2$ , and  $f_1$  can sense different short-circuit currents. Whether it is open-circuit voltage or short-circuit current, great linearity was observed. Based on the linearity of the induced value, one can use this characteristic as multi-state applications.

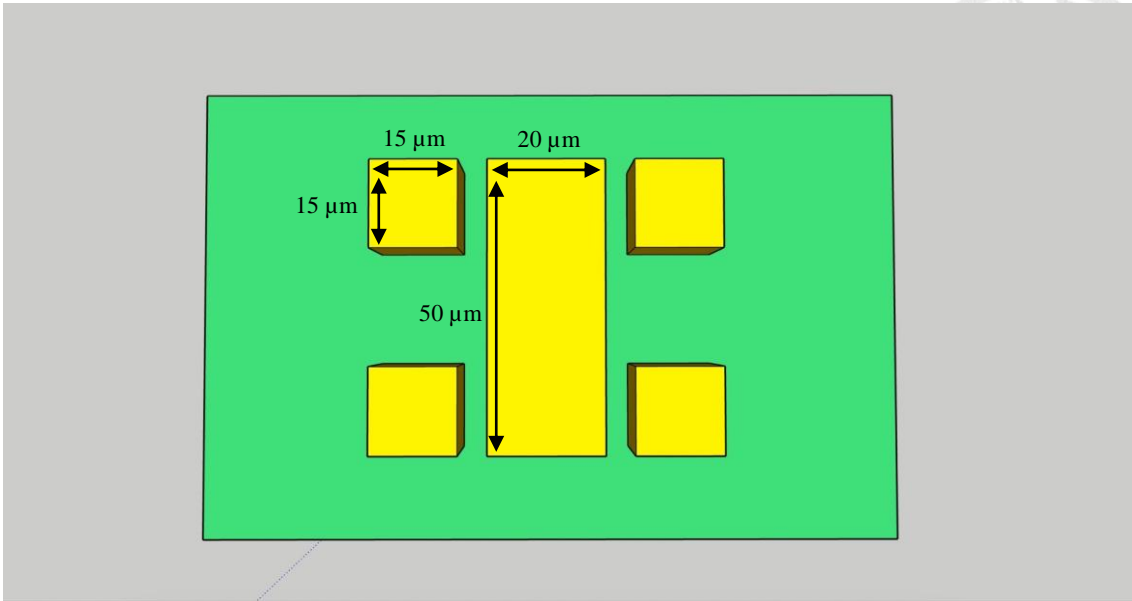


Fig. 2-1. Schematic top view of the 4 rings MIS TD device.

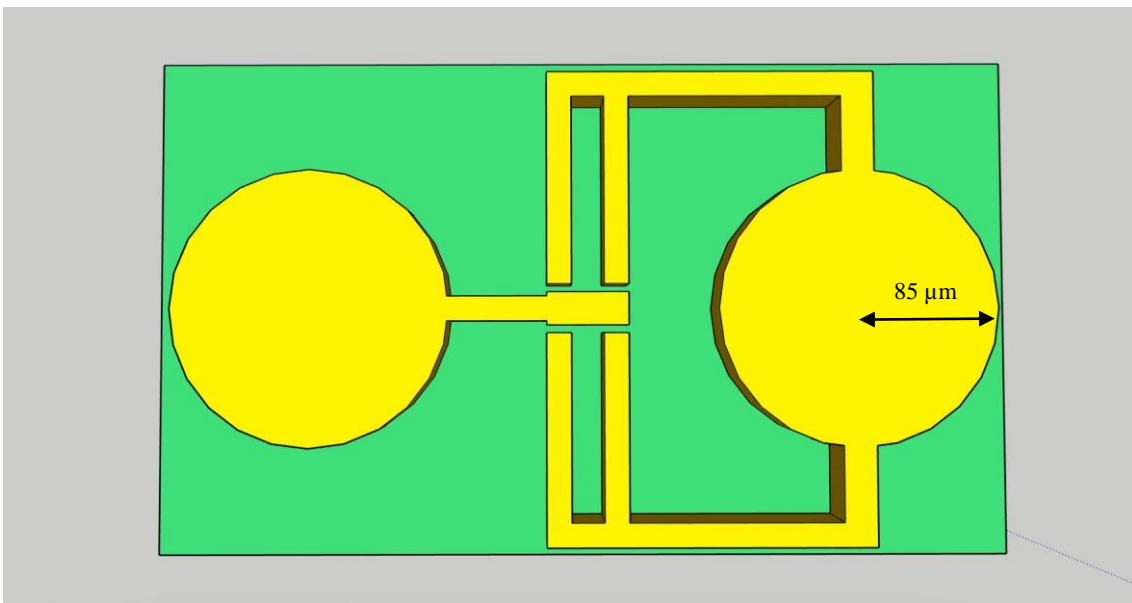


Fig. 2-2. Schematic top view of the 4 rings MIS TD device with circular pad.

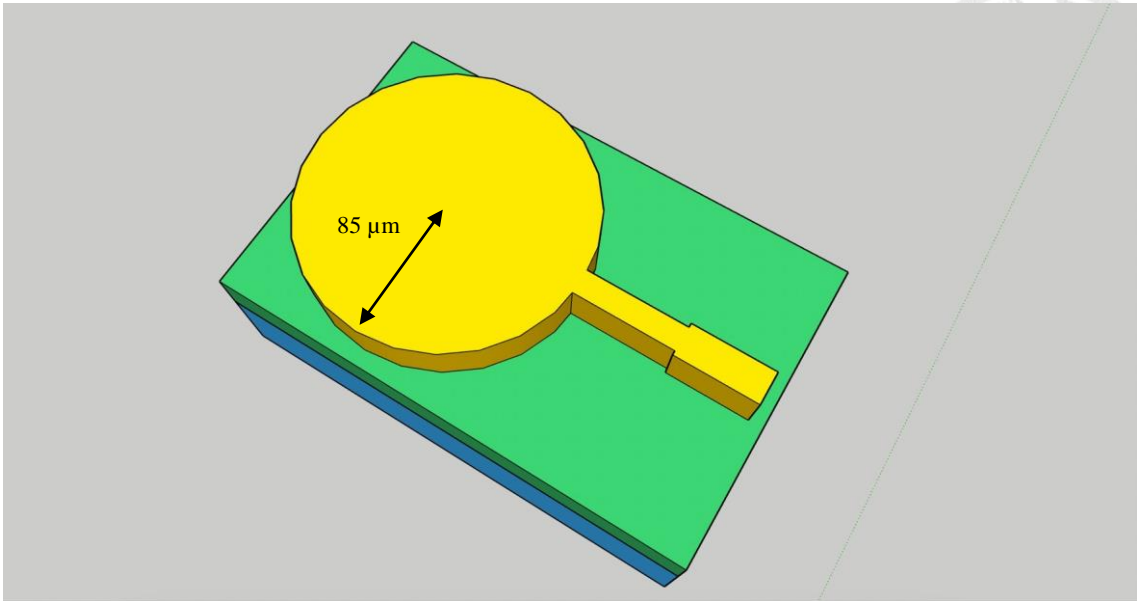


Fig. 2-3. Schematic top view of the center MIS TD device.

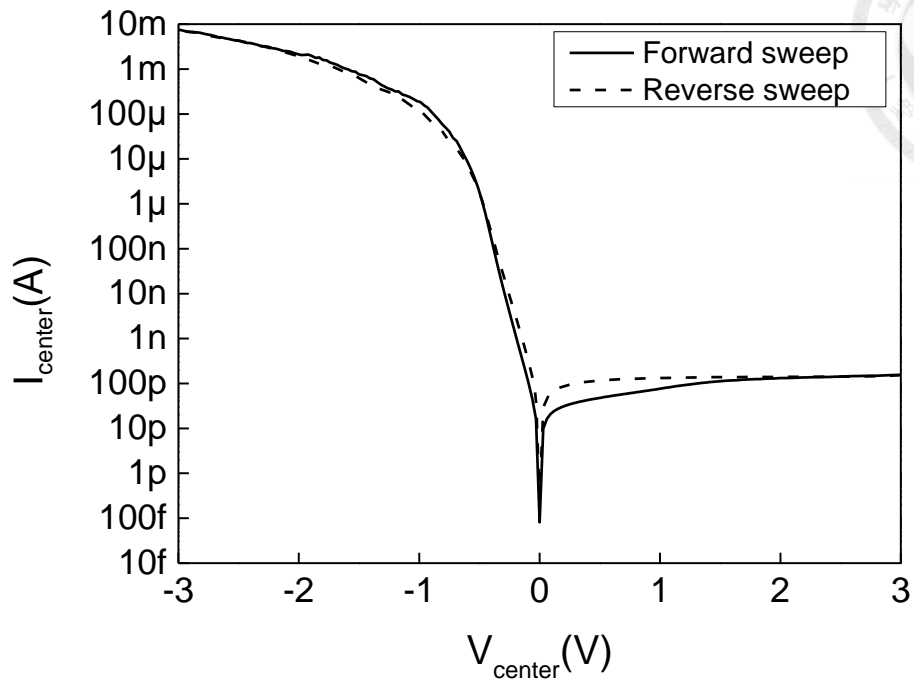


Fig. 2-4. I-V curves of the center MIS TD.

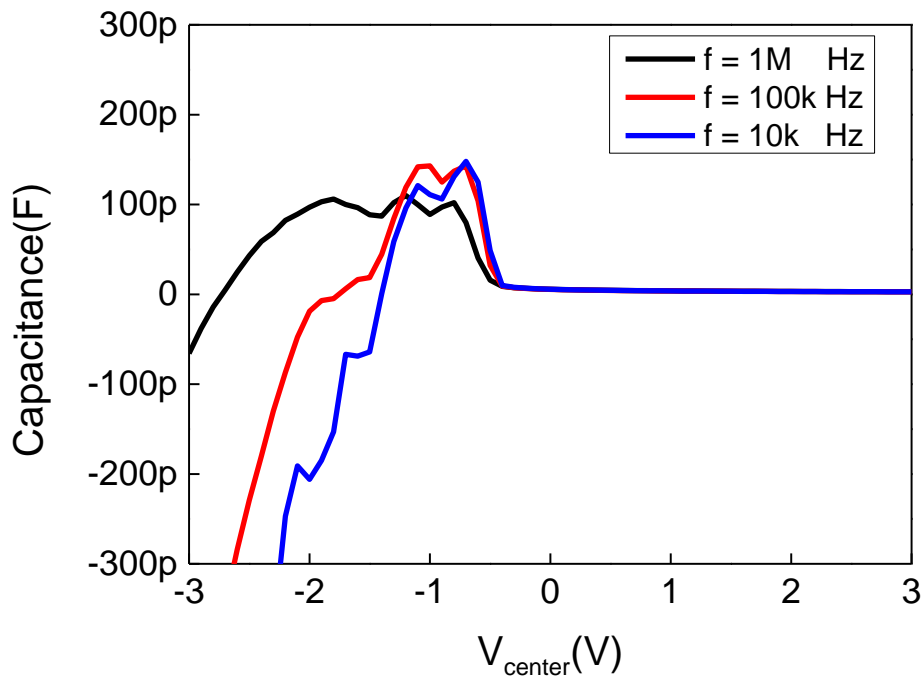
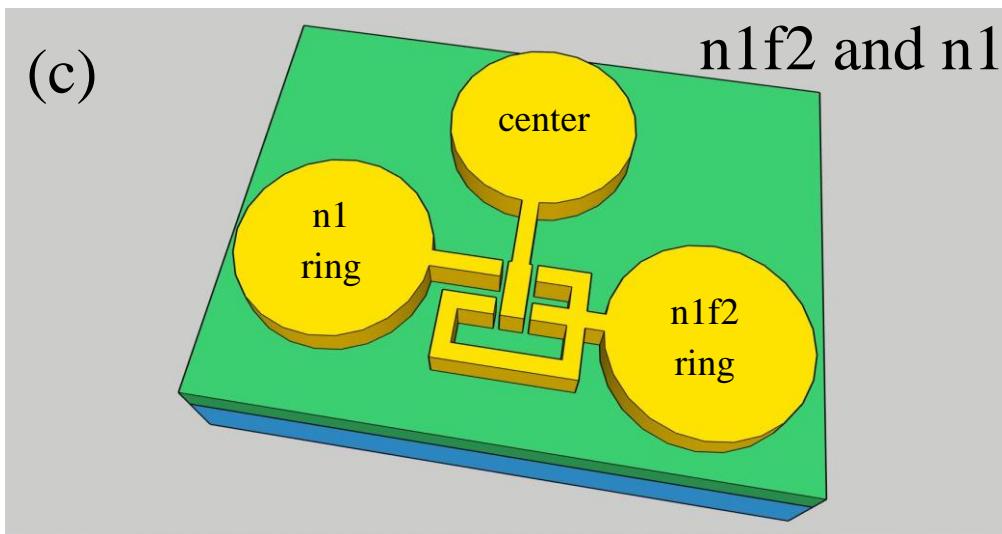
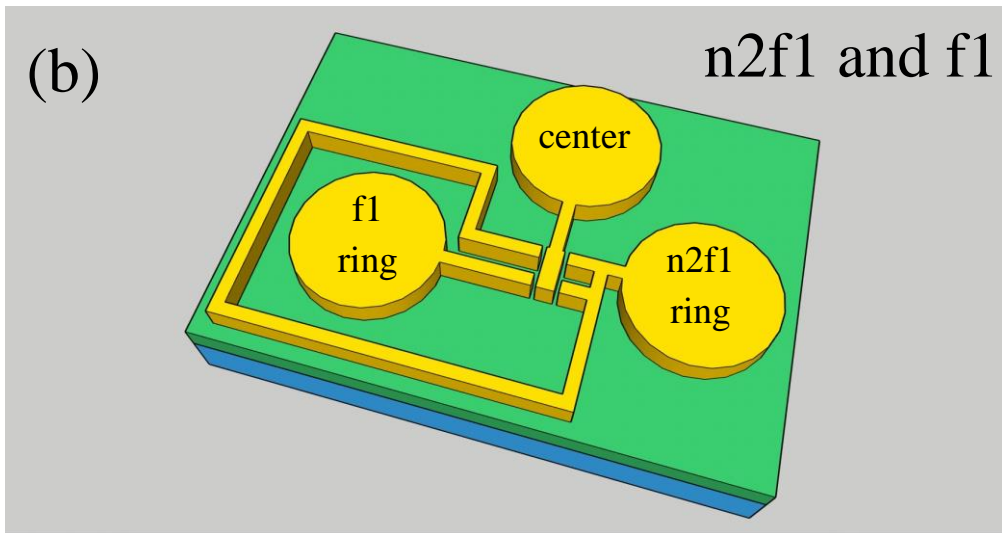
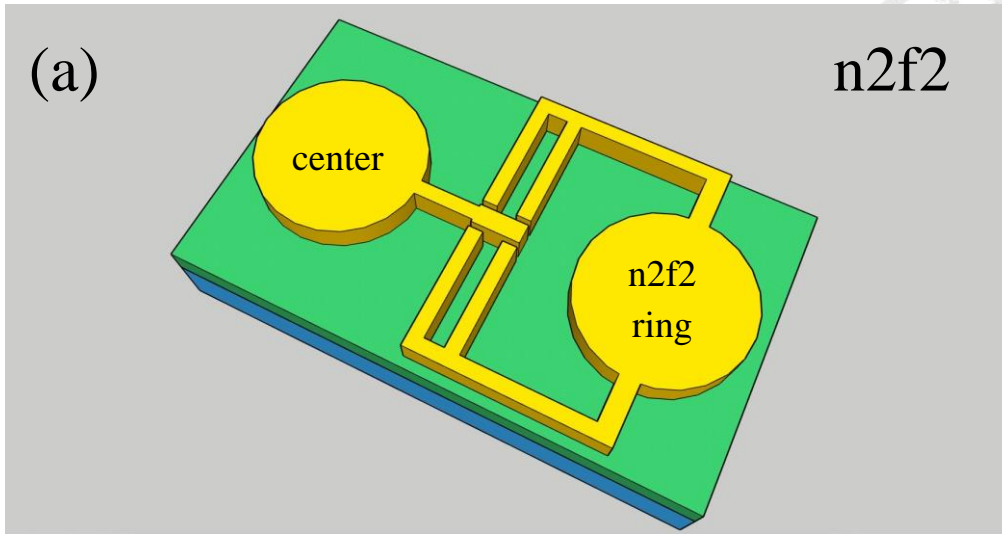


Fig. 2-5. C-V curves of the center MIS TD.



(to be continued)

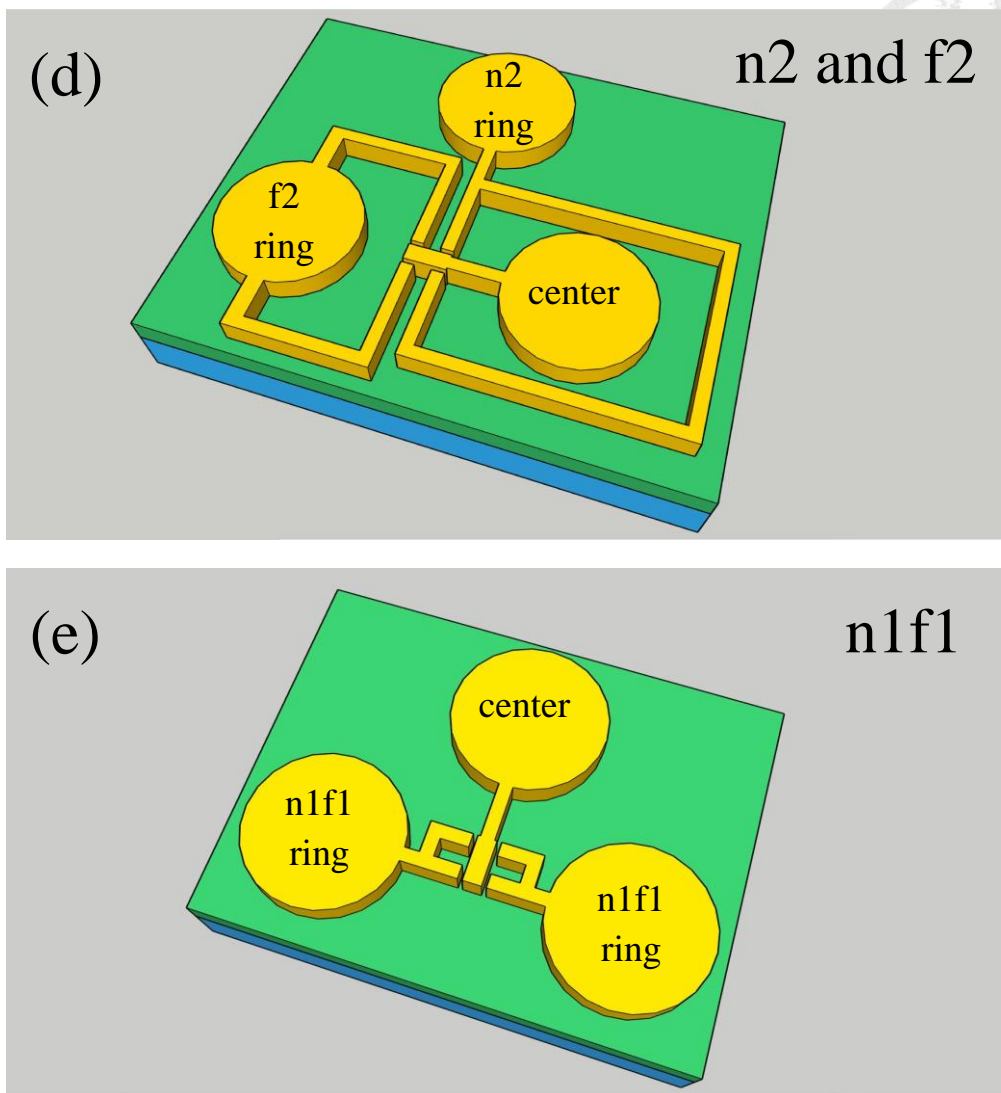


Fig. 2-6. 3D schematic top view of (a) the 4 rings (n2f2), (b) the 3 rings (n2f1) and the 1 ring (f1), (c) the 3 rings (n1f2) and the 1 ring (n1), (d) the 2 rings (n2) and (f2), and (e) the 2 rings (n1f1) MIS TD devices. n means near and f means farther.



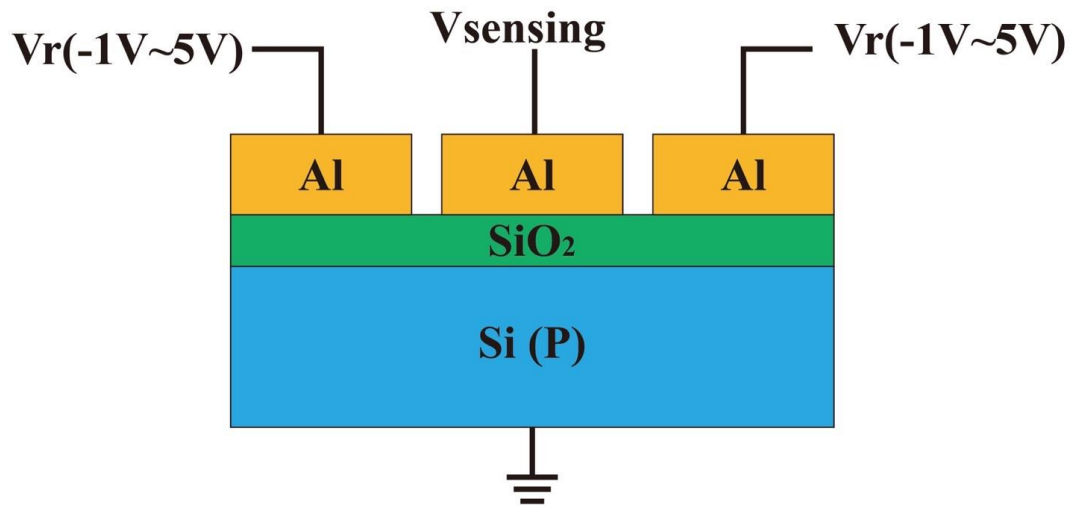
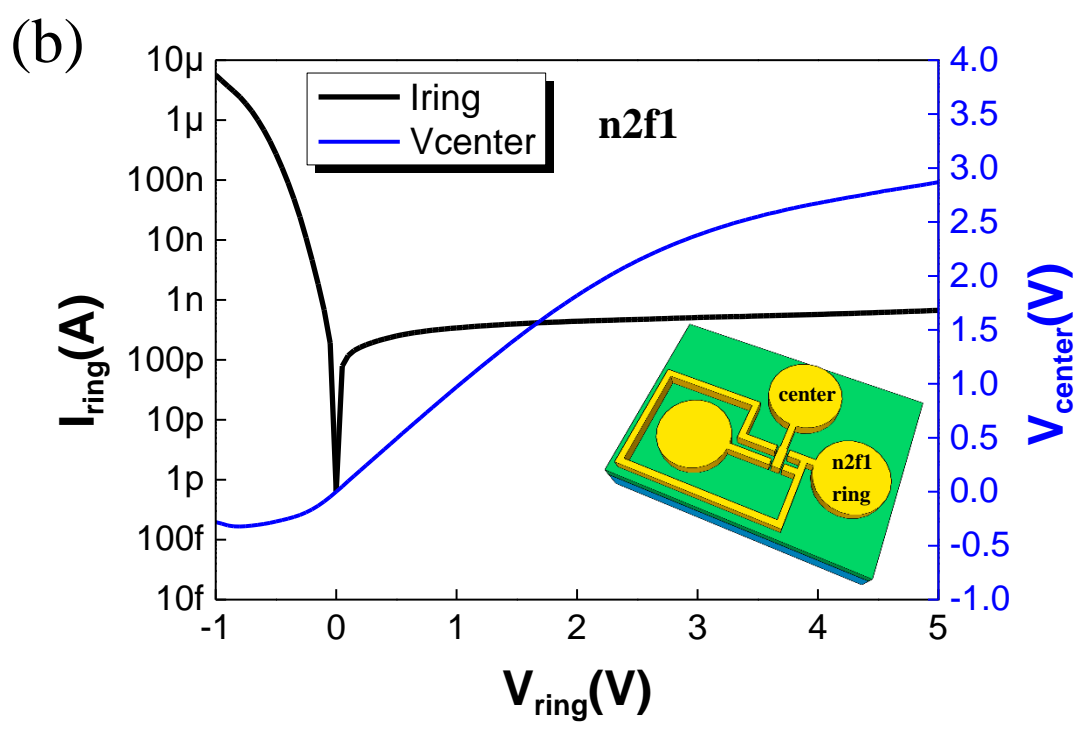
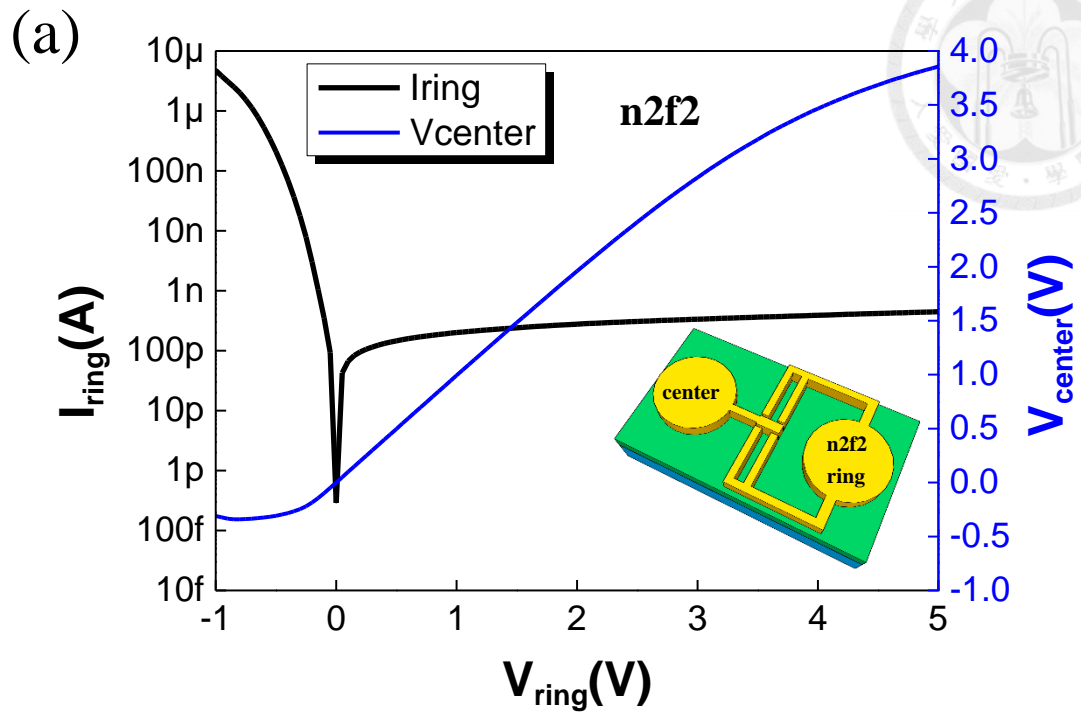
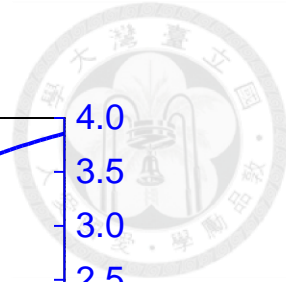
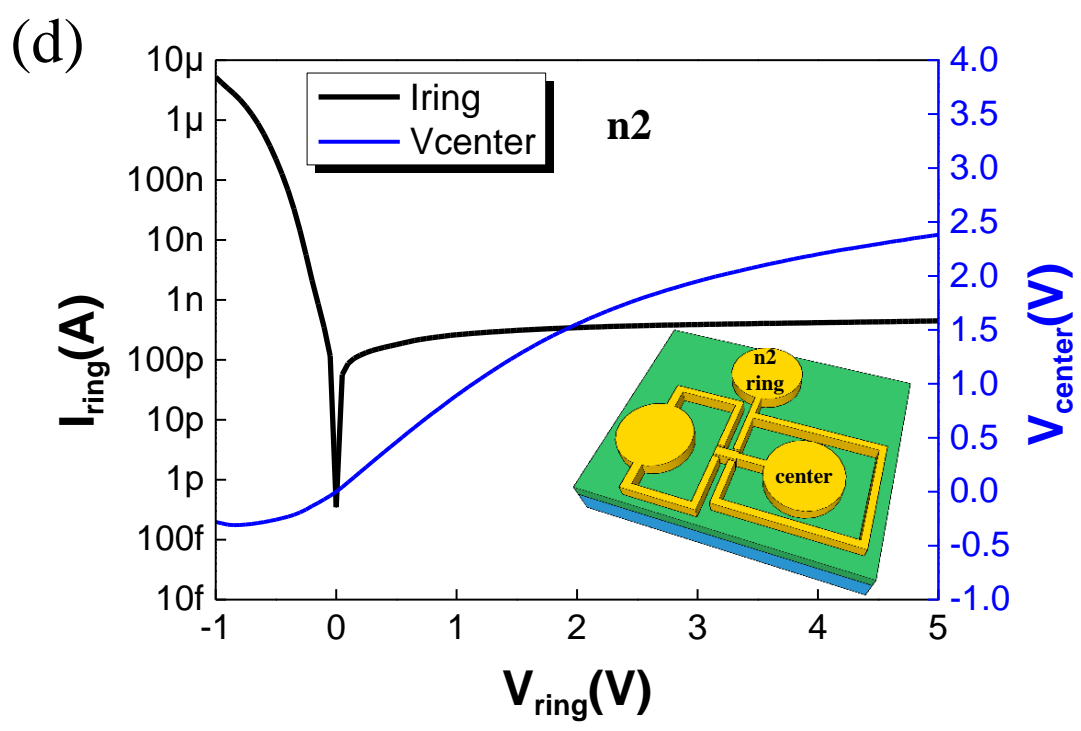
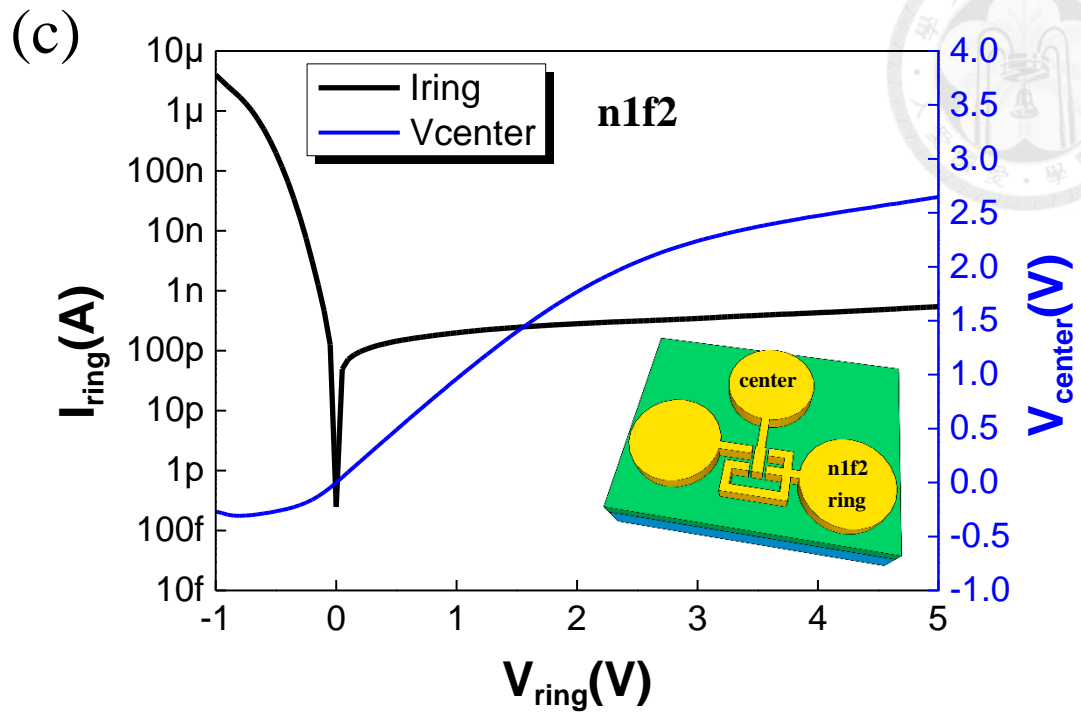
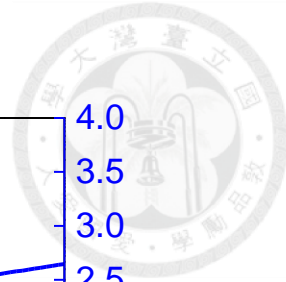


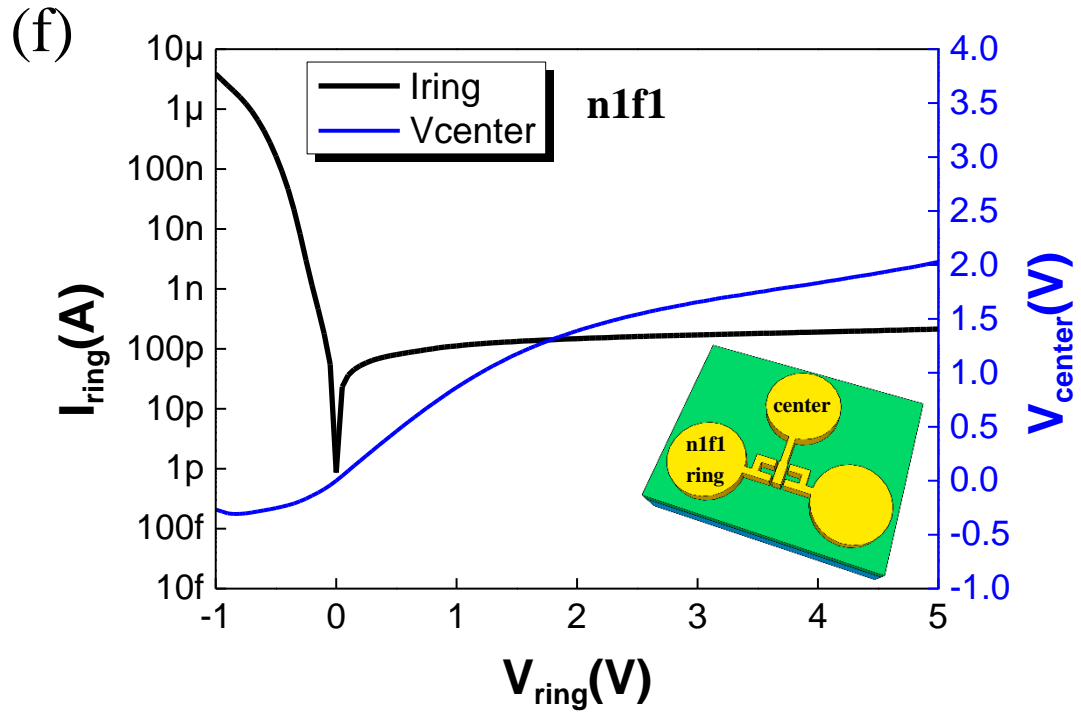
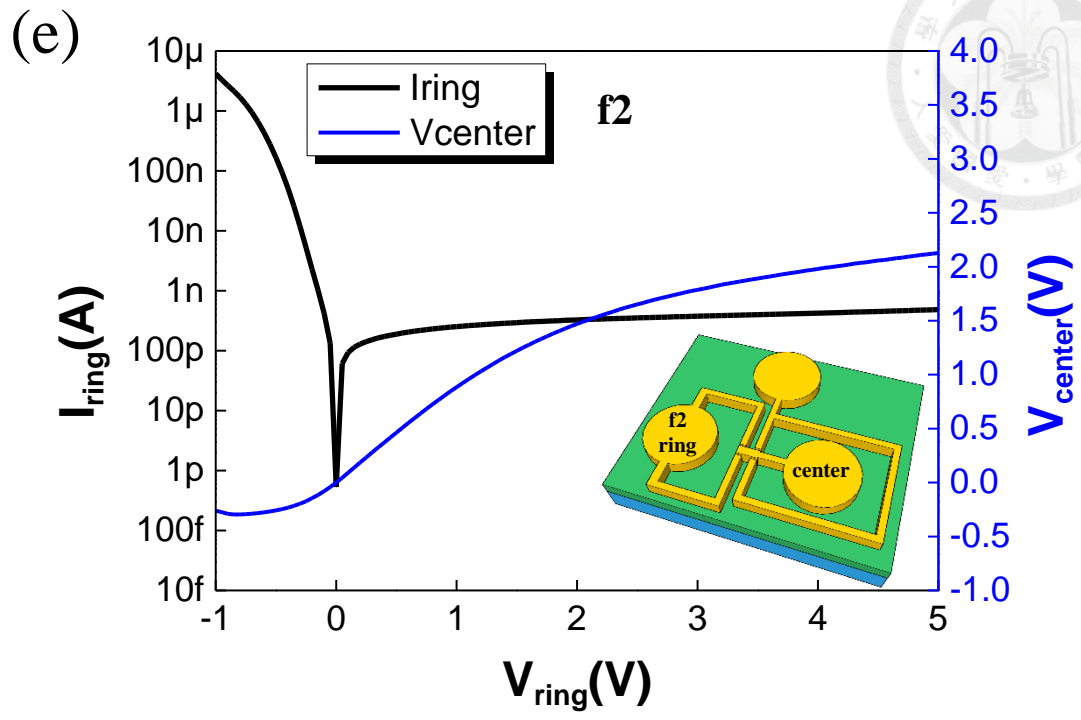
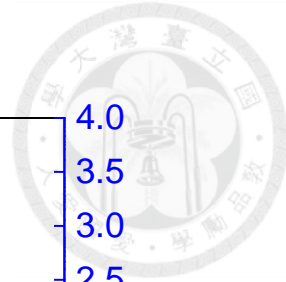
Fig. 2-7. Schematic of open-circuit voltage operation.



(to be continued)



(to be continued)



(to be continued)

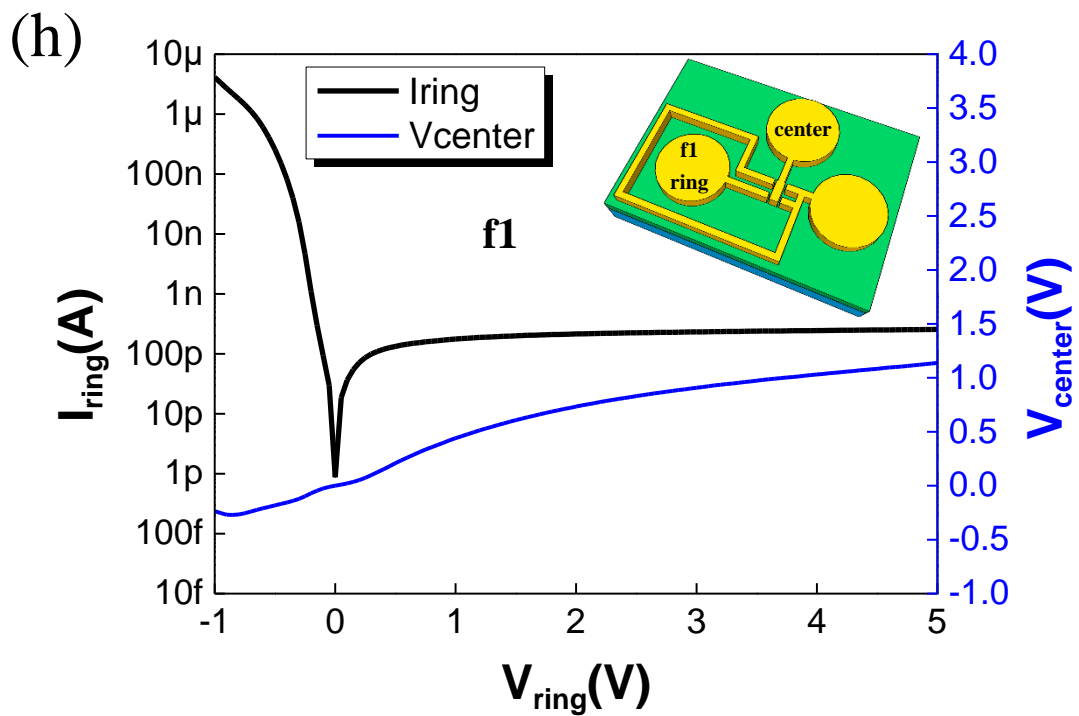
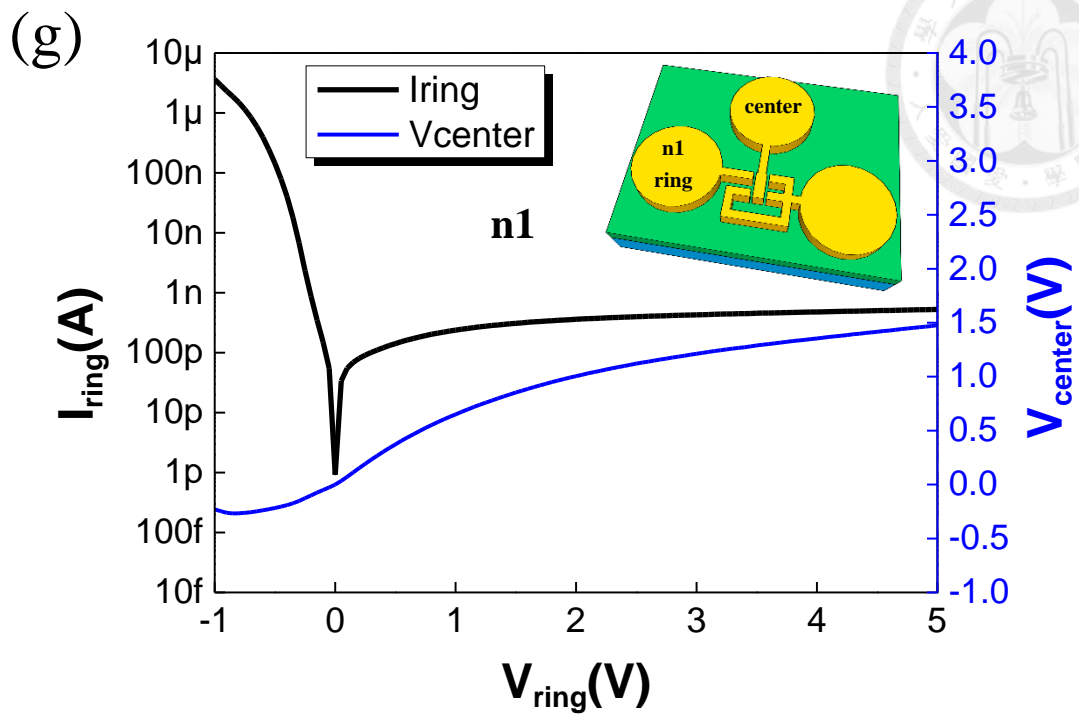


Fig. 2-8.  $I_{ring}$  &  $V_{center}$  versus  $V_{ring}$  curves of (a) the 4 rings (n2f2), (b) the 3 rings (n2f1), (c) the 3 rings (n1f2), (d) the 2 rings (n2), (e) the 2 rings (f2), (f) the 2 rings (n1f1), (g) the 1 ring (n1), and (h) the 1 ring (f1) MIS TD devices.

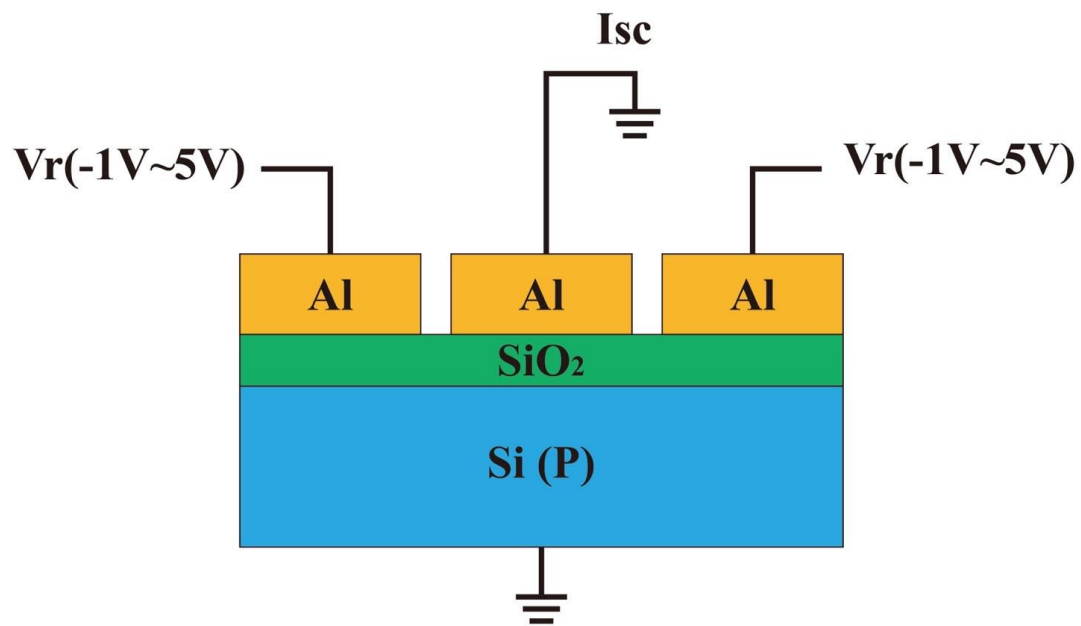
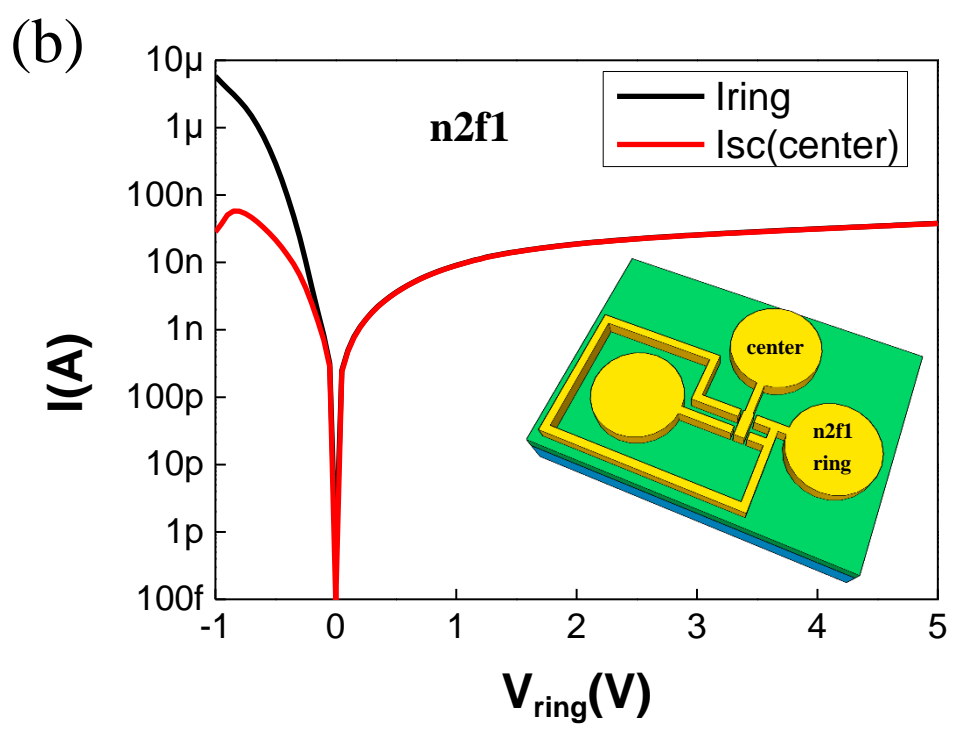
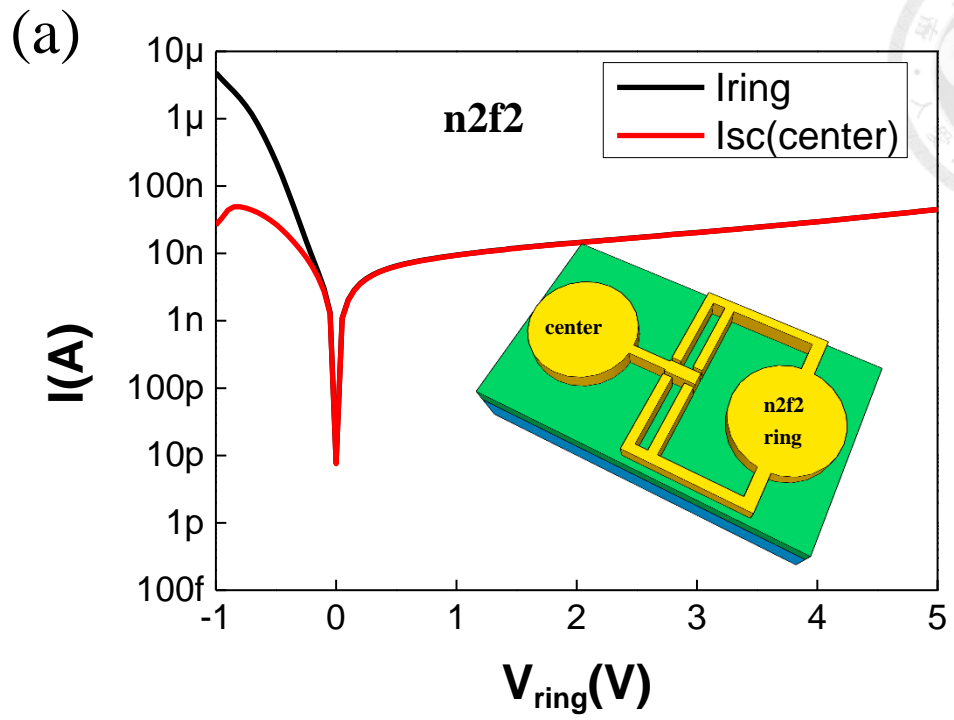
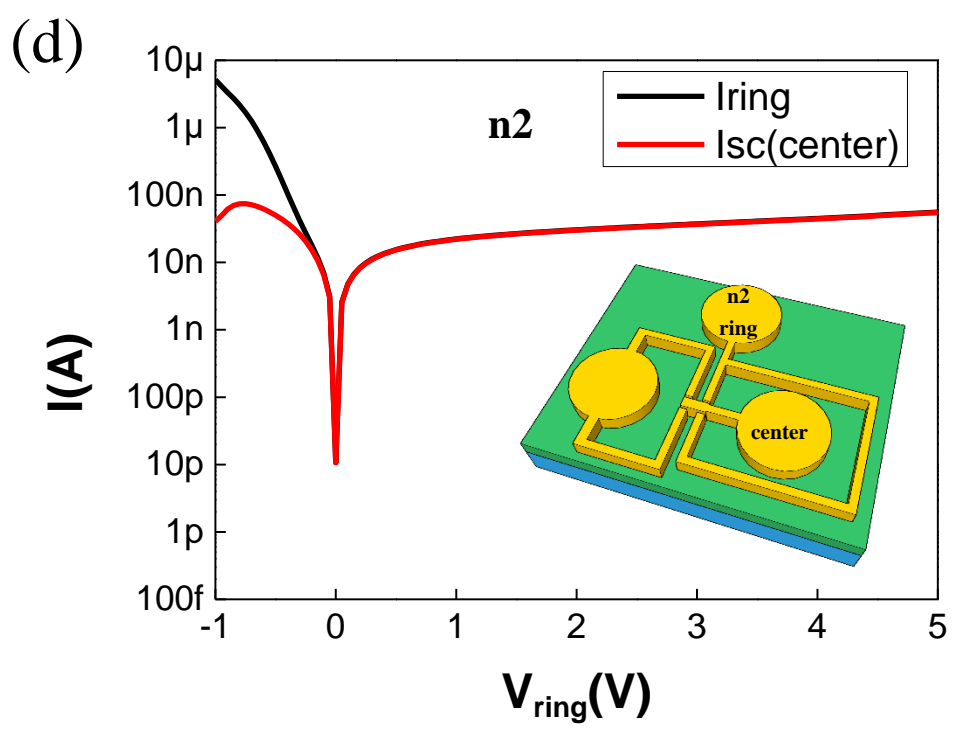
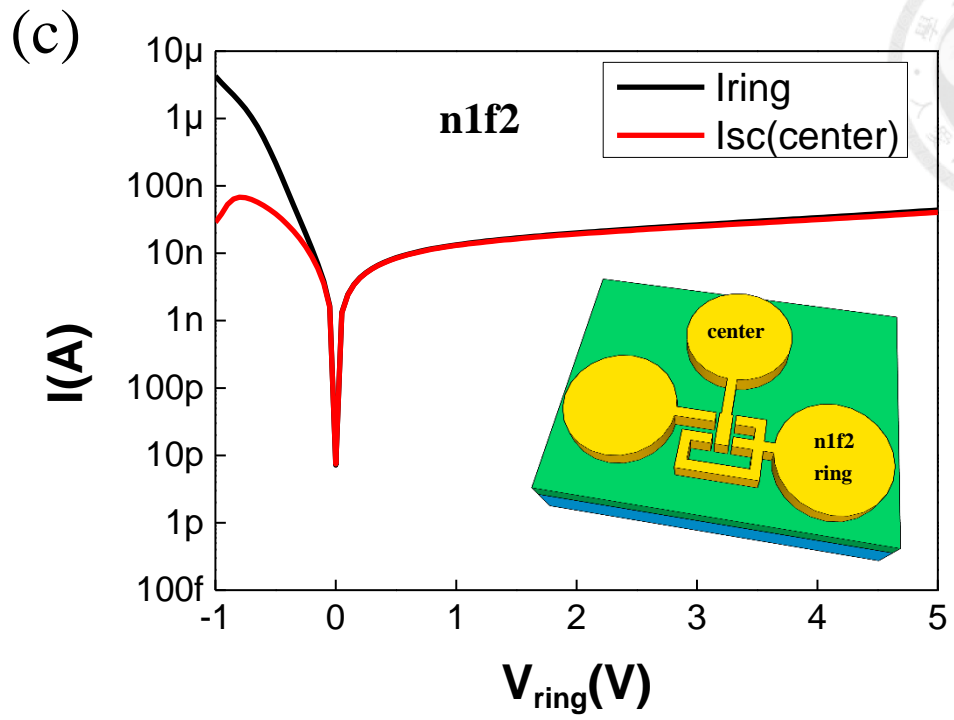


Fig. 2-9. Schematic of short-circuit current operation.

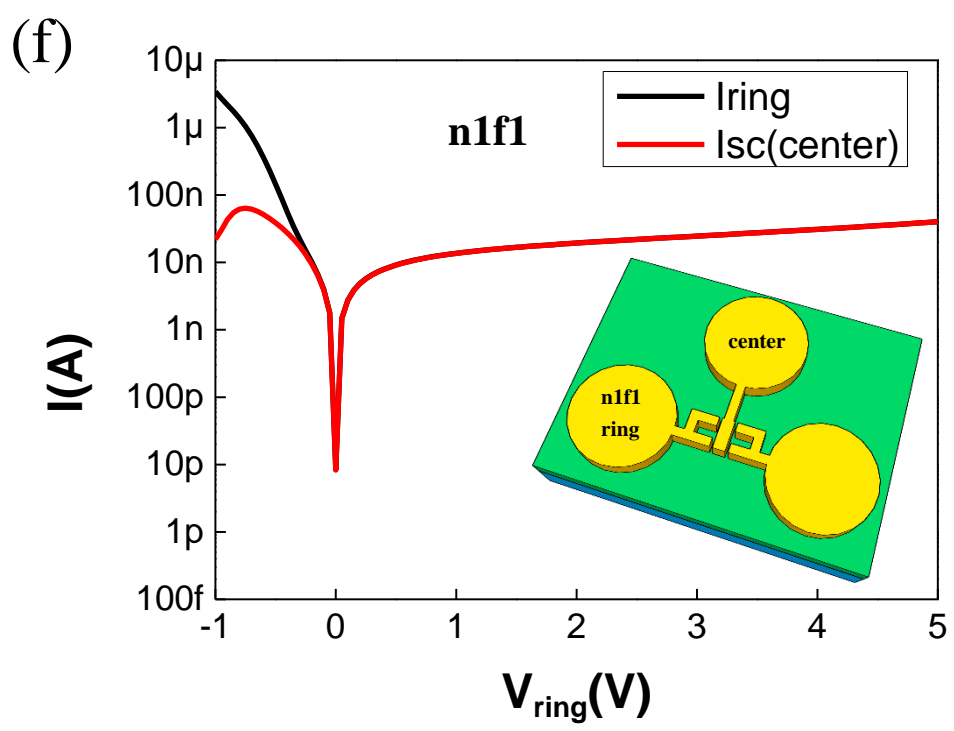
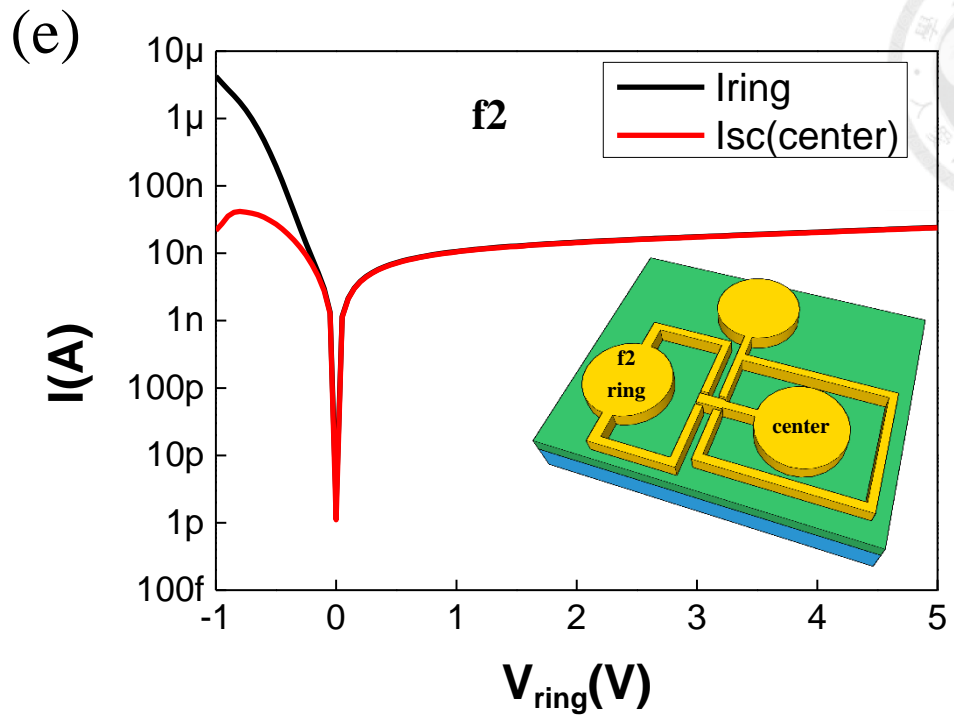


(to be continued)



(to be continued)





(to be continued)

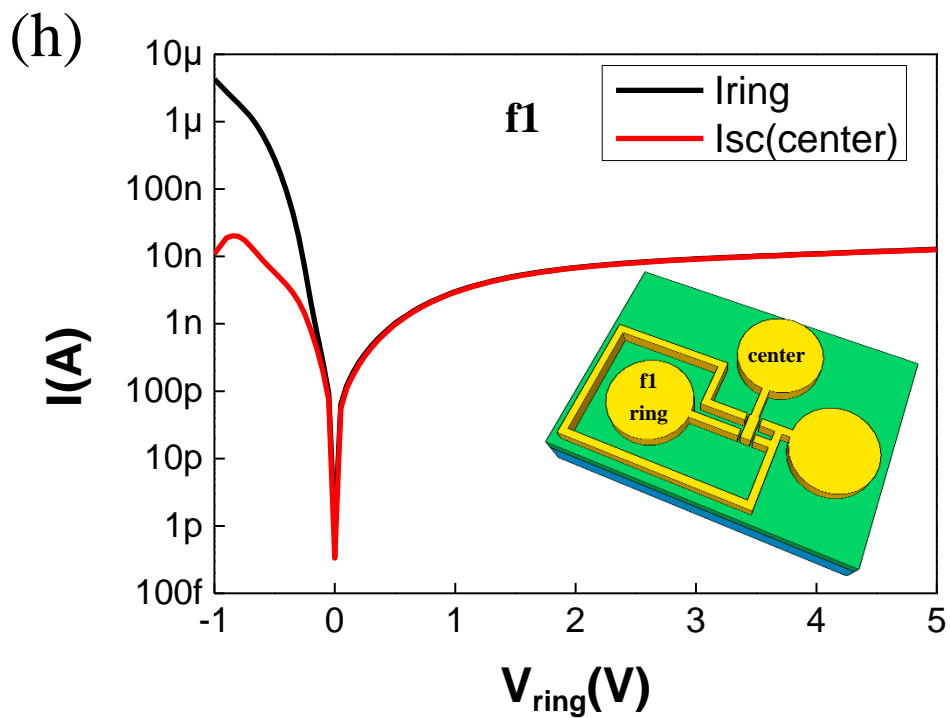
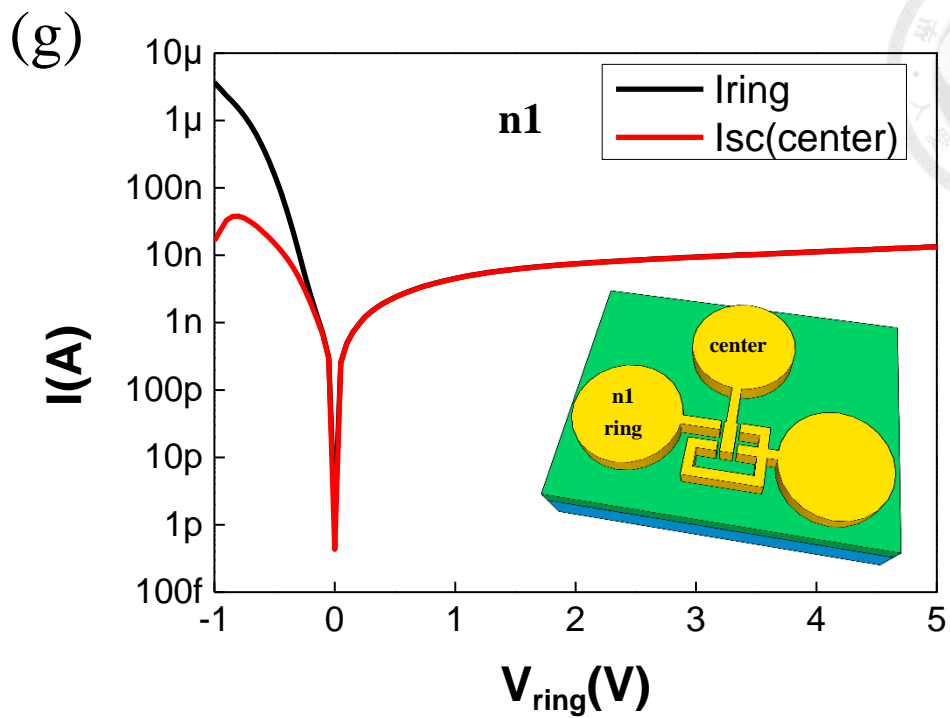


Fig. 2-10.  $I_{\text{ring}}$  &  $I_{\text{sc}(\text{center})}$  versus  $V_{\text{ring}}$  curves of (a) the 4 rings (n2f2), (b) the 3 rings (n2f1), (c) the 3 rings (n1f2), (d) the 2 rings (n2), (e) the 2 rings (f2), (f) the 2 rings (n1f1), (g) the 1 ring (n1), and (h) the 1 ring (f1) MIS TD devices.

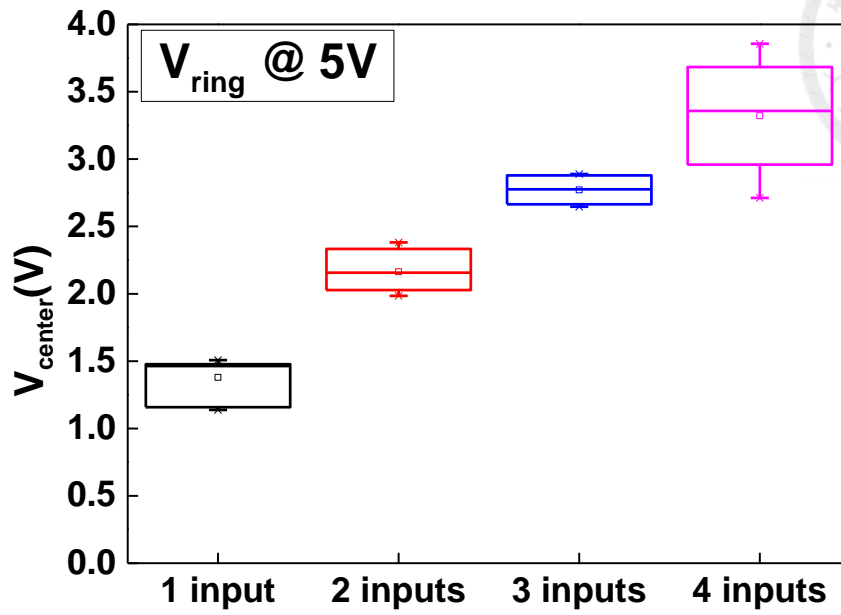


Fig. 2-11. Error bar chart of coupling open-circuit voltages with different inputs.

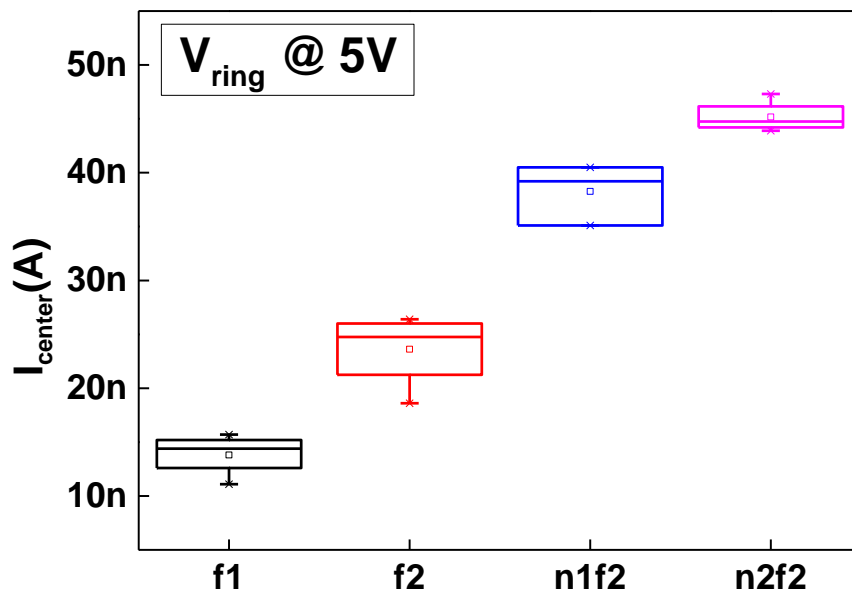


Fig. 2-12. Error bar chart of coupling short-circuit currents with different devices.



## **Chapter 3**

# **Coupling Effect of High-Low Structure**

# **MIS TD Enhanced by Novel Soft**

# **Breakdown Operation**

### **3-1 Introduction**

### **3-2 Experimental Procedure**

### **3-3 Results and Discussions**

#### **3-3-1 I-V Characteristics in Planar and High-Low Structure**

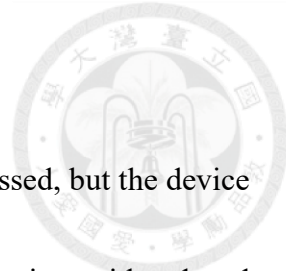
#### **3-3-2 Soft Breakdown Mechanism in High-Low Device**

#### **3-3-3 Ring Soft Breakdown Induced by Center with Negative bias**

#### **3-3-4 Electric Field and Electron Concentration in TCAD**

### **Simulation**

### **3-4 Summary**

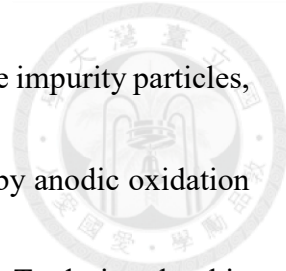


### 3-1 Introduction

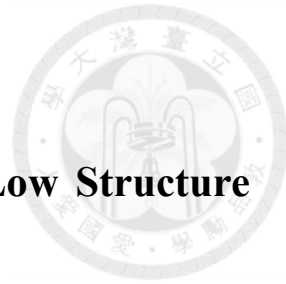
In **Chapter 2**, MIS TD with multiple outer rings has been discussed, but the device size is too large to be compatible with the modern technology node. Devices with reduced size and their characteristics are further discussed. The method of shrinking device size is achieved by using the high-low oxide process. It is to grow thick oxide first, and then grow thin oxide. When the device changes from the planar to high-low, the characteristics will be different. When operating in the reverse bias, since the region of thick oxide layer will provide extra minority carriers to the region of thin oxide layer, the inversion current will not be saturated, which is different from the planar device. If the inversion current is not saturated, there is no way to achieve the requirement of low power consumption and the wanted coupling effect between the ring and the center. Therefore, we propose a method to make the inversion current saturated by using special soft breakdown process. To achieve the best performance, the soft breakdown with current compliance and induced bias voltage will be used to make the coupling effect between the ring and the center to the best. Finally, the electric field distribution of the induced soft breakdown can be proven by SILVACO TCAD simulation.

### 3-2 Experimental Procedure

A boron-doped 1-10  $\Omega$ -cm (100) p-type silicon wafer was used as the substrate. At



first, we use standard Radio Corporation of America (RCA) to remove impurity particles, native oxide and organic impurities. A thick oxide layer was grown by anodic oxidation in D.I. water and the oxide layer thickness was about 24.7 nm [11]. To design the thin oxide region on device, we defined the pattern by photolithography and wet etching. Then a thin oxide layer was grown by anodic oxidation in D.I. water and the oxide layer thickness was about 2.3 nm [11]. The above steps are the process of thick first and then thin, which produces high-low oxide layer. Rapid thermal process at 950°C for 15 seconds was used for post-oxidation annealing. Then 200 nm Al film was deposited on the oxide layer by thermal evaporation. To achieve the electron pattern on device, we defined the pattern by photolithography and wet etching. The top view of the device was shown in Fig. 3-1. The central region is a rectangle and the size is 50  $\mu\text{m}$   $\times$  20  $\mu\text{m}$ . The outer region are four squares and the size are all 15  $\mu\text{m}$   $\times$  15  $\mu\text{m}$ . Both of these are connected to a circular pad with a radius of 85  $\mu\text{m}$  as shown in Fig. 3-2. Here, we named the central region as center and the outer region as ring. Center and ring are located in the thin oxide layer, while the connected circular pad is located in the thick oxide layer. Finally, the back oxide was removed by buffered oxide etch (BOE). A 250 nm Al film was evaporated on the back side as back contact. The electrical characteristics and analysis were measured by Agilent B1500A in dark environment.



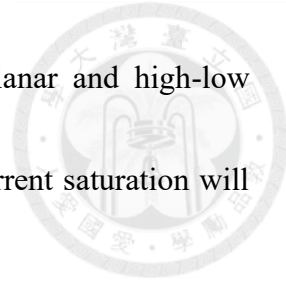
## 3-3 Results and Discussion

### 3-3-1 I-V Characteristics in Planar and High-Low Structure

#### Operations

The characteristics of the center region of planar structure and high-low structure are compared in the beginning. Planar structures can be divided into thin oxide and thick oxide. Thin oxide has been discussed in **Chapter 2**. In the reverse bias, the current will be saturated and is extremely low, which can be used as a multi-state device. For thick oxide, because the oxide layer is very thick, the measured current is almost the displacement current. Therefore, it can be seen from Fig. 3-3 that the forward/reverse sweep currents exhibit significant hysteresis and will not be saturated. The main structure of this chapter is the high-low oxide device, Fig. 3-4 shows the top view of the high-low center device. In Fig. 3-5, the current has a slight hysteresis phenomenon, but the current value is not as low as planar structure of thick oxide. The current will increase linearly with the increase of voltage, because the region of thick oxide layer will continuously provide extra minority carriers to thin oxide region. Although the center is located in the thin oxide region, the connected circular pad is in the thick oxide region. Therefore, there will be a continuous supply of minority carriers from thick oxide region to thin oxide region, so the current will not be saturated under the reverse bias, and the coupling effect

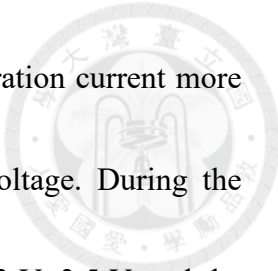
cannot be achieved. Fig. 3-6 is the I-V curves comparison of planar and high-low structures. The method of using special soft breakdown to reach current saturation will be discussed next.



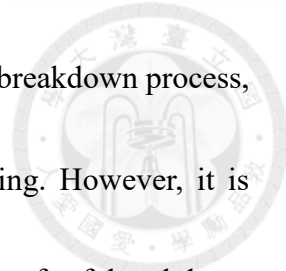
### **3-3-2 Soft Breakdown Mechanism in High-Low Device**

Soft breakdown can be thought of as punching an aisle in the oxide layer, which will be called OLT (oxide local thinning) [6]. After the OLT is formed, minority carriers will be replenished through the OLT under the reverse bias. Because of the high tunneling rate of the OLT due to pinch-off effect, the number of carriers will be limited instead of continuously replenishing from the thick oxide region. Hence, the current will be saturated. There are many ways to make the device to soft breakdown. Here are two methods, the first is to apply stress on the device to break through the oxide layer. For example, 6 V with 10 seconds can be applied to the center and the ring. Of course, the applied bias voltage and stress time can be adjusted. The method of applying stress can easily cause the saturation current of the device to be too large after a soft breakdown, which we do not expect. The second method is sweeping bias at the center and the ring. For example, sweeping the voltage of -1 V~5 V at the center and ring, when the current of forward sweep and reverse sweep have a significant jump and saturation, that means there is a soft breakdown on the device. In this chapter, the method of sweeping current





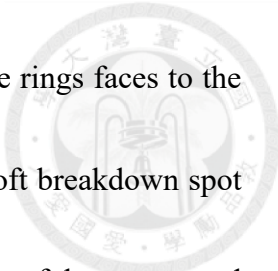
to achieve soft breakdown is conducted. In order to control the saturation current more concisely, there will be current compliance when sweeping the voltage. During the measurement, it was found that soft breakdown will occur at about 3 V~3.5 V, and the current is about 100 nA. Hence, we set the current compliance to 100 nA and the sweeping range is from 0 V to 3.5 V. That is to say, when the current value is equal to 100 nA and the soft breakdown will be occur, and keep continuing to sweep the voltage after the soft breakdown will not cause further damage because of the current compliance. The above operation can better control the degree of soft breakdown. Experiments have found that if there is only a soft breakdown of the center, or only a soft breakdown of the outer rings, there will be no coupling effect between the two. It is therefore believed that both of them must be soft breakdown to exhibit a coupling device. In this experiment, the center will perform the operation of soft breakdown first and then the outer rings will continue the operation of soft breakdown. Fig. 3-7(a) is the soft breakdown operation of the center region. The first step is to sweep -1 V~2 V to confirm that the device is not soft breakdown. The second step is the operation of soft breakdown that sweeping 0 V~3.5 V and set a current compliance of 100 nA. The third step is to measure the characteristics of -1 V~4 V after the soft breakdown. After the center being soft breakdown, the outer rings is then to be soft breakdown with the same operation. Fig. 3-7(b) is the soft breakdown operation



of the ring region. After both the center and the ring finished the soft breakdown process, the device will have coupling effect between the center and the ring. However, it is expected that the coupling effect is hard to control because the regions of soft breakdown are random.

### **3-3-3 Ring Soft Breakdown Induced by Center with Negative Bias**

In order to further make the coupling effect and coupling voltage more stable, here we propose a novel idea of induced soft breakdown. After the soft breakdown operation of center, a bias of -1 V was applied to the center when the ring was carried out the process of soft breakdown at the same time. This method is to make the electric field distribution uneven. It is believed that the OLT of the center is located at the border around the center. The reason is that the surrounding electric field is larger due to the fringing field effect, so the probability of center's edge being soft breakdown is higher. The closer the distance between the soft breakdown regions of center and the ring, the better the coupling effect. The best way is to make two soft breakdown spots be as close as possible. It is known that the magnitude of the electric field will affect the probability of soft breakdown. When the soft breakdown process was conducted on the ring with -1 V applied to the center, the ring region which to closer to the soft breakdown spot of the center will sustain a larger



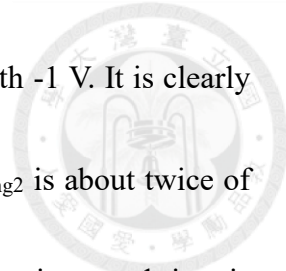
electric field. That is to say, when there are 4 rings around, one of the rings faces to the soft breakdown spot of center will have the largest electric field. A soft breakdown spot of the ring will occur at the position closest to the soft breakdown spot of the center, and two soft breakdown spots will be closet. Fig. 3-8(a) is the soft breakdown operation of the center and Fig. 3-8(b) shows that the ring soft breakdown operation with -1 V applied to the center. The devices stabilities are compared in Fig. 3-9(a) and Fig. 3-9(b) for samples without and with a voltage of -1V applied to the center during ring soft breakdown operation. It is noticed that the coupling voltage of the ring was used as the sensing parameter in this figure. It is obvious that the coupling voltage without -1 V is very unstable. Even at  $V_c = 2$  V and  $V_c = 1.75$  V, the coupled  $V_{ring}$  has a staggered phenomenon, which means that the coupling effect is not excellent, and it cannot be used as a multi-state device; but the coupling voltage with applying -1 V to the center is very stable, and the  $V_{ring}$  obtained by different  $V_c$  is obviously different. The coupled voltage is larger than the case without -1 V, so it means that the coupling effect is stronger. It is clear that the device is operated by using the center as the input and the ring as the sensor. That is to say, a bias voltage was applied to the center, and then the open-circuit voltage of the ring was read. It can be seen in the Fig. 3-10(a)~(d) that the voltages sensed by 4 rings, 3 rings, 2 rings and 1 ring are different. At  $V_c = 4$  V, the corresponding coupled

$V_{ring}$  are approximately 3.33 V, 2.81 V, 2.66 V, and 2.46 V. Therefore, the high-low oxide structure also have the potential to be multi-state devices by using the novel soft breakdown method be used as proposed in this work.

### **3-3-4 Electric Field and Electron Concentration in TCAD**

#### **Simulation**

To verify the above expectation about the enhanced electric field in ring due to certain OLT and applied bias in center, SILVACO TCAD simulation will be used. The first thing to simulate is that the soft breakdown of the center will be occur around the center's edge. The Fig. 3-11 is a schematic of the simulation device for planar oxide. The parameters obtained are that the thickness of the oxide layer is about 2.3 nm, the width of ring1 & ring2 are equal to 15  $\mu\text{m}$ , the width of center is 20  $\mu\text{m}$ , both  $V_{r1}$  and  $V_{r2}$  are 0 V, and  $V_c = 5$  V, and set the cutline to be 2 nm below the top of the oxide layer. The magnitude of the electric field looks similar in the center in Fig. 3-12(a), but when we zoom in that region one can find the electric field at the edge of the center ( $x = -10 \mu\text{m}$  &  $x = 10 \mu\text{m}$ ) will be greater than the electric field inside the device in Fig. 3-12(b). The reason is that there will be a fringing field near the device's edge, resulting in the soft breakdown spot will probably occur at the center's edge. Next, we assume that there is an OLT on the edge of the center ( $x = 8.5 \sim 9 \mu\text{m}$ ) as shown in Fig. 3-13. Both ring<sub>1</sub> and ring<sub>2</sub> were



applied with the same bias voltage of 3 V and center was applied with -1 V. It is clearly that the electric field of ring<sub>2</sub> is larger than ring<sub>1</sub> in Fig. 3-14(a).  $E_{\text{ring}2}$  is about twice of  $E_{\text{ring}1}$ , so ring<sub>2</sub> is more likely to have a chance of soft breakdown than ring<sub>1</sub>, and ring<sub>2</sub> is also closer to the OLT of the center, which can make the two OLTs as close as possible. Thus, the coupling effect is better and more stable. Similarly, if we apply a bias voltage of 4 V or 5 V at ring<sub>1</sub> and ring<sub>2</sub>, we can also clearly see the difference in the electric field of ring<sub>1</sub> and ring<sub>2</sub> in Fig. 3-14(b) and Fig. 3-14(c). In addition to the electric field, the electron concentration is also of importance and is related to the electric field. In Fig. 3-15, it can be seen that the electron concentration distribution of ring<sub>2</sub> is higher than ring<sub>1</sub> with  $V_{r1} = V_{r2} = 3 \text{ V} / V_c = -1 \text{ V}$ , so the electric field is relatively large. These simulations are in line with expected assumption. Next, we set a bias voltage of  $V_{\text{set}@I=0} = V_{\text{oc}(\text{coupled})} = 0.425 \text{ V}$  and  $V_{r1} = V_{r2} = 5 \text{ V}$ , to simulate the center to approach the floating state condition. In the Fig. 3-16(a) and Fig. 3-16(b), the electric field magnitude and electron concentration between ring<sub>1</sub> and ring<sub>2</sub> are almost the same. The probability of soft breakdown between the two is about the same, and the location of the soft breakdown is random. If one set the positive bias of  $V_c = 3 \text{ V}$  and  $V_{r1} = V_{r2} = 5 \text{ V}$ , the electric field and electron concentration between ring<sub>1</sub> and ring<sub>2</sub> are still similar as shown in Fig. 3-17(a) and Fig. 3-17(b). Therefore, only when a negative bias voltage was applied to the center,

the electric field of ring<sub>1</sub> and ring<sub>2</sub> can be non-uniform.



### 3-4 Summary

**Chapter 3** focuses on the design of high-low oxide structure in order to reduce the device area to be compatible with the current technology nodes. However, the thick oxide region will provide extra minority carriers to the thin oxide region, and therefore the current cannot reach saturation in the reverse bias and the device can't display coupling effect. It is necessary to use soft breakdown to improve the device coupling characteristics. But, soft breakdown by applying stress or sweeping voltage may make the saturation current too large, and the coupling effect is not well controlled. Therefore, we propose novel methods of soft breakdown. The current compliance is limited to 100 nA during the soft breakdown operation of center, and when ring is under soft breakdown operation, not only the current is limited to 100 nA, but also -1 V is applied to the center. So the soft breakdown spot of the ring can be controlled at the position close to the soft breakdown spot of the center. Finally, the novel soft breakdown can reduce the saturation current in the reverse bias, and the coupled voltages of 4 rings, 3 rings, 2 rings and 1 ring can also display multi-state characteristics.

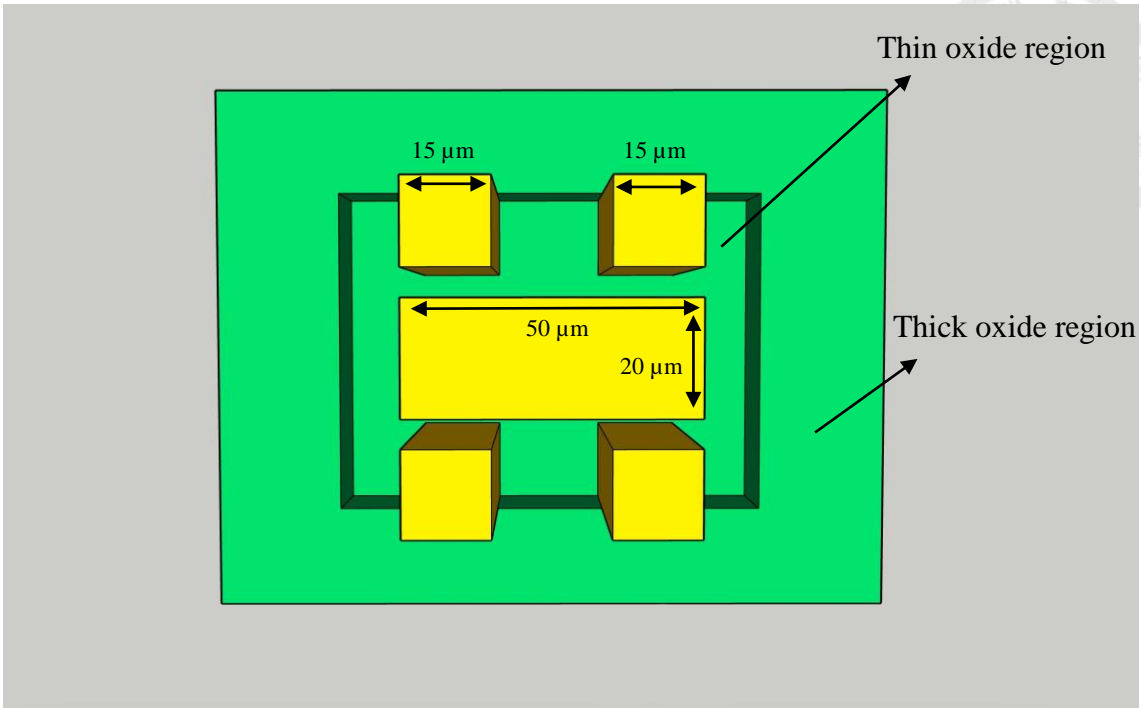


Fig. 3-1. Schematic top view of the high-low center MIS TD device.

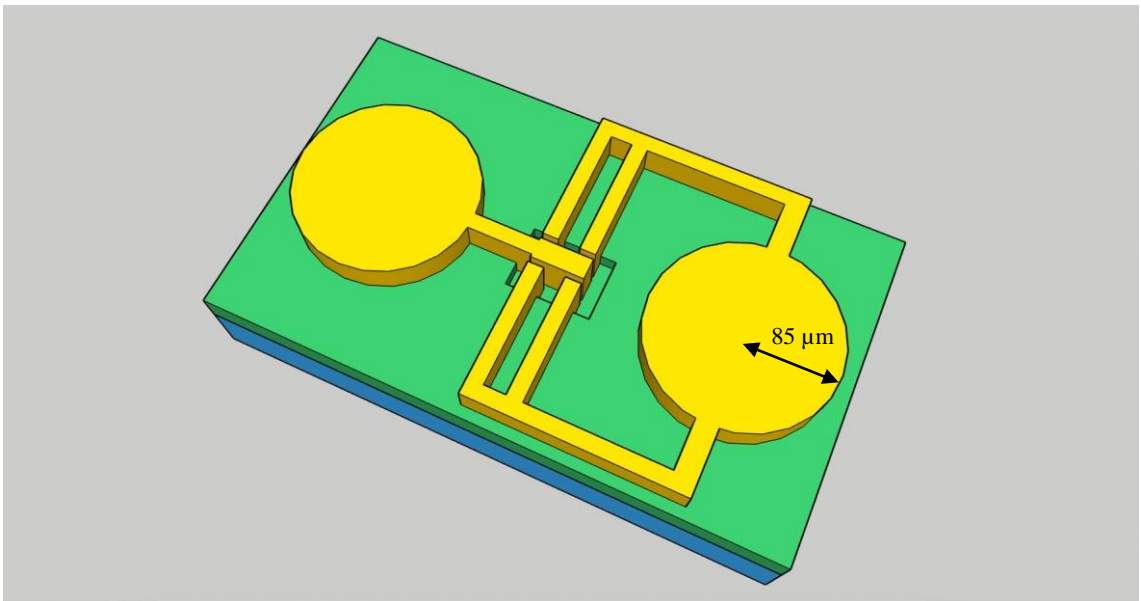


Fig. 3-2. Schematic top view of the 4 rings high-low MIS TD device with circular pad.

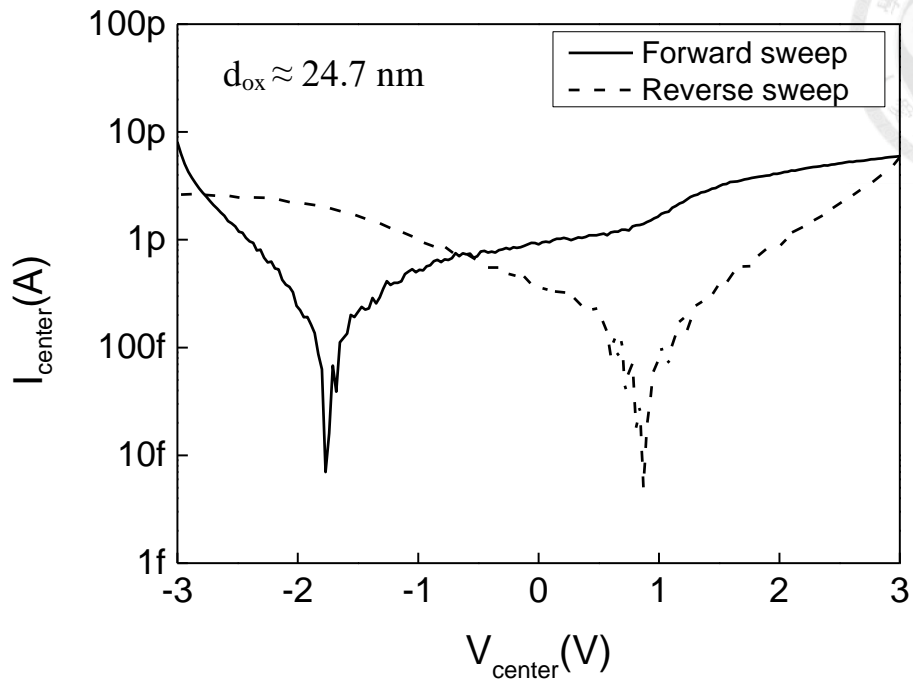


Fig. 3-3. I-V curves of the thick oxide center MIS TD.



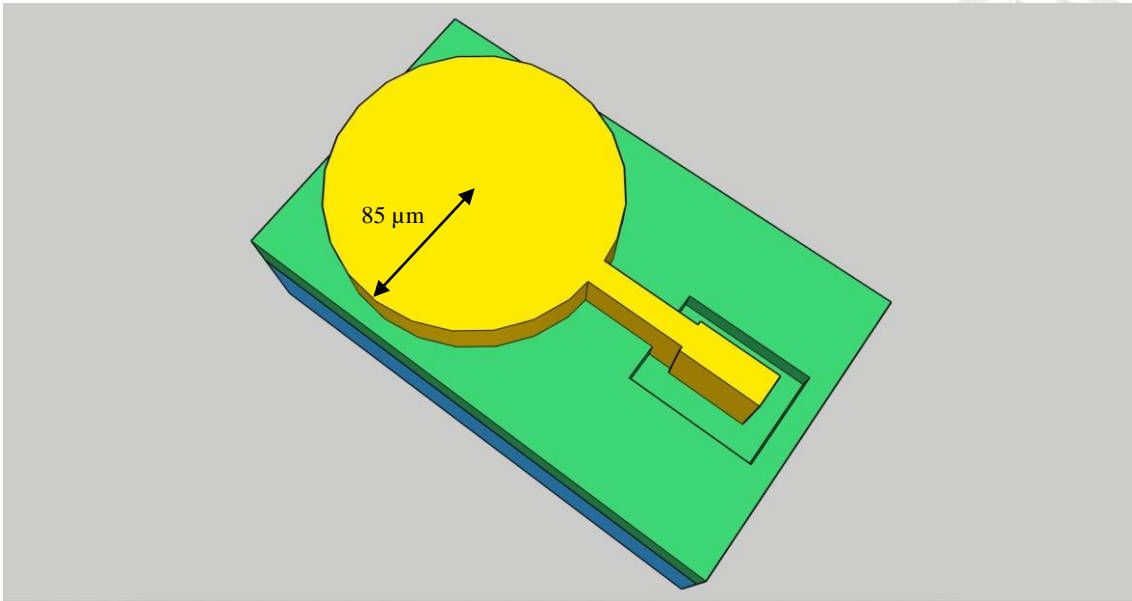


Fig. 3-4. 3D Schematic top view of the high-low center MIS TD device.

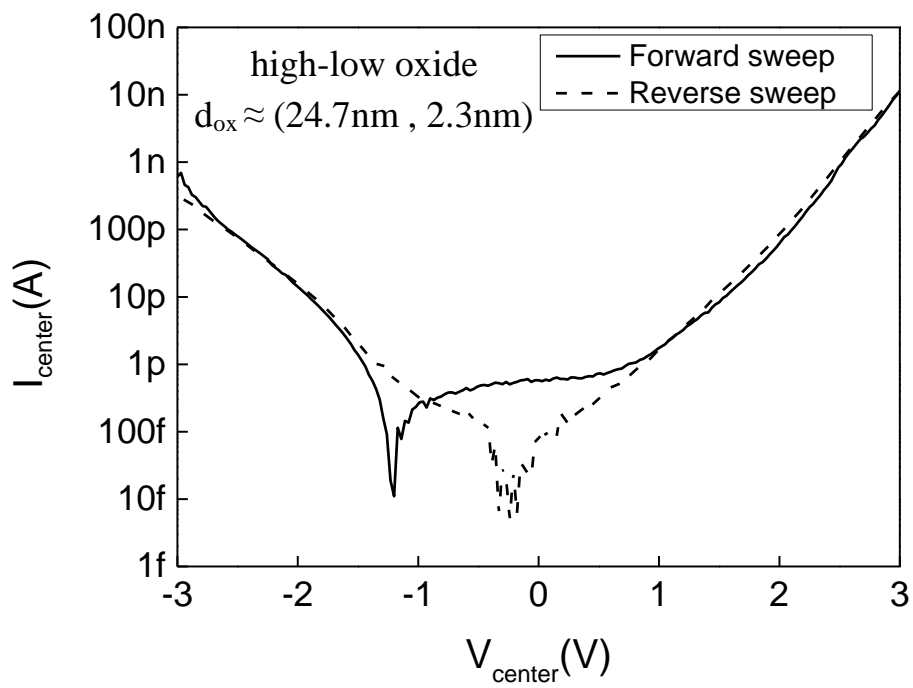


Fig. 3-5. I-V curves of the high-low oxide center MIS TD.

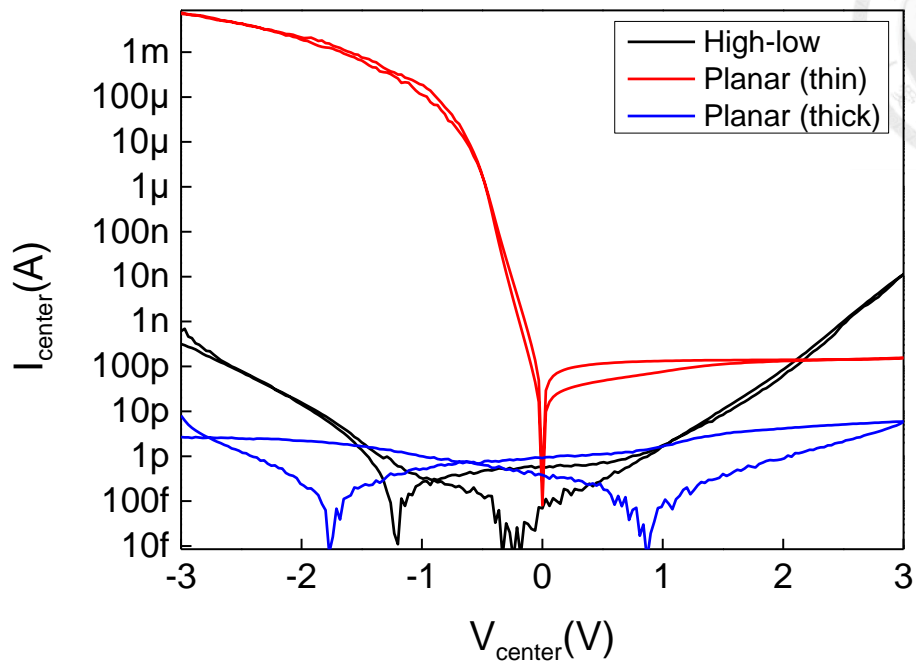


Fig. 3-6. I-V curves of the planar and high-low center MIS TD.

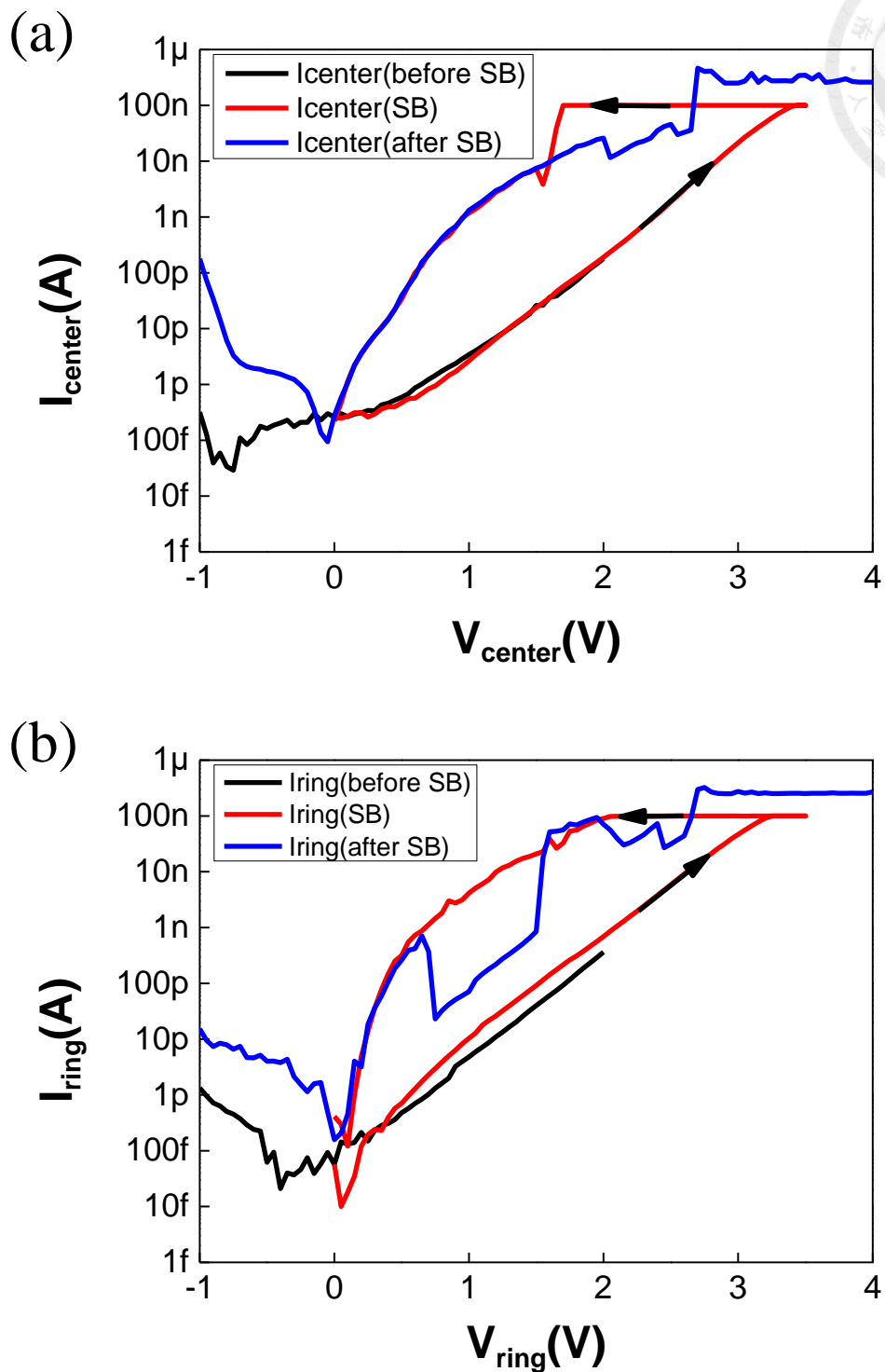


Fig. 3-7. I-V curves of (a) the center MIS TD with soft breakdown operation and (b) the 4 rings MIS TD with proceeded soft breakdown operation.

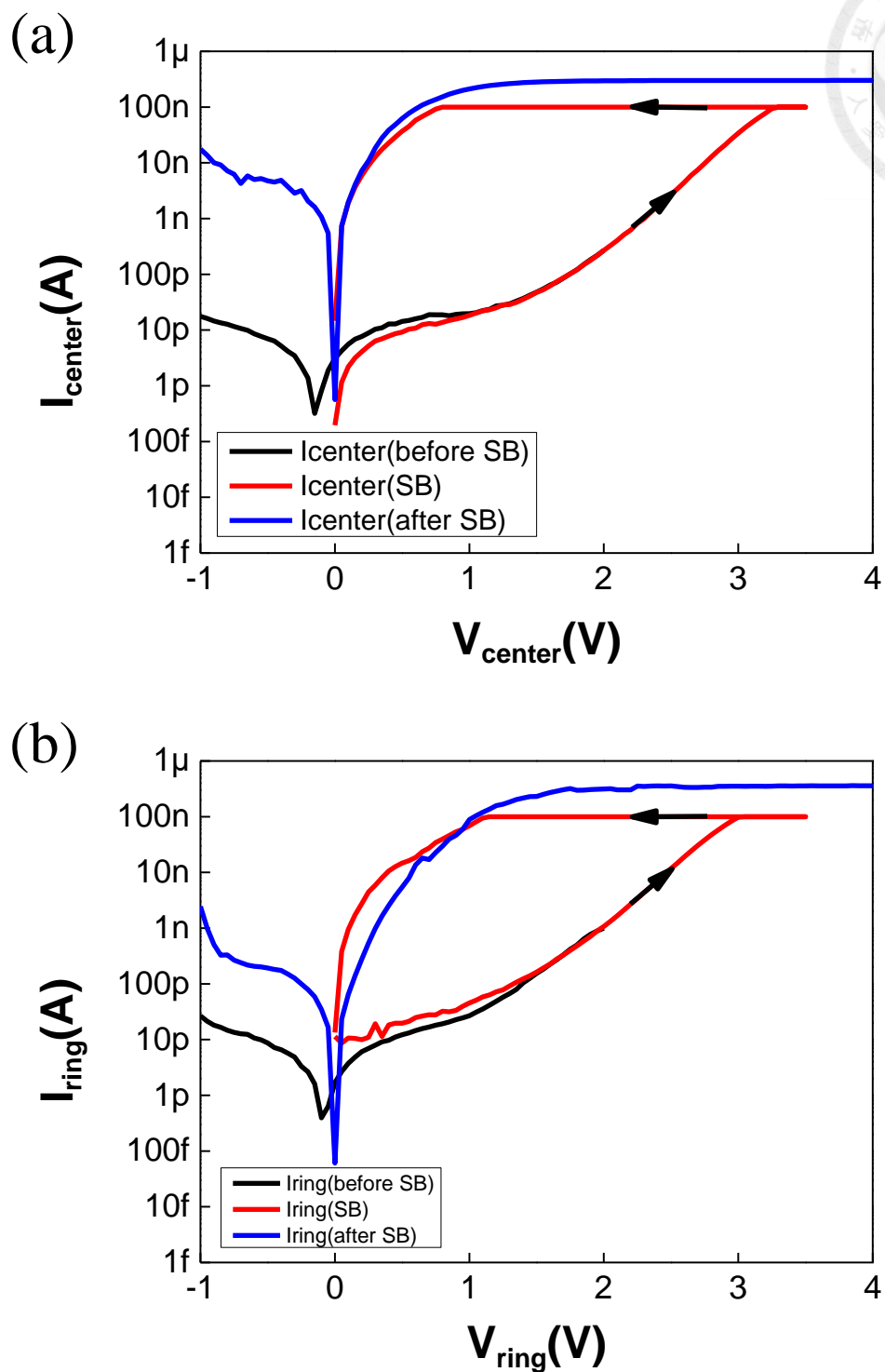


Fig. 3-8. I-V curves of (a) the center MIS TD with soft breakdown operation and (b) the 4 rings MIS TD with proceeded soft breakdown operation with -1 V applied to the center.

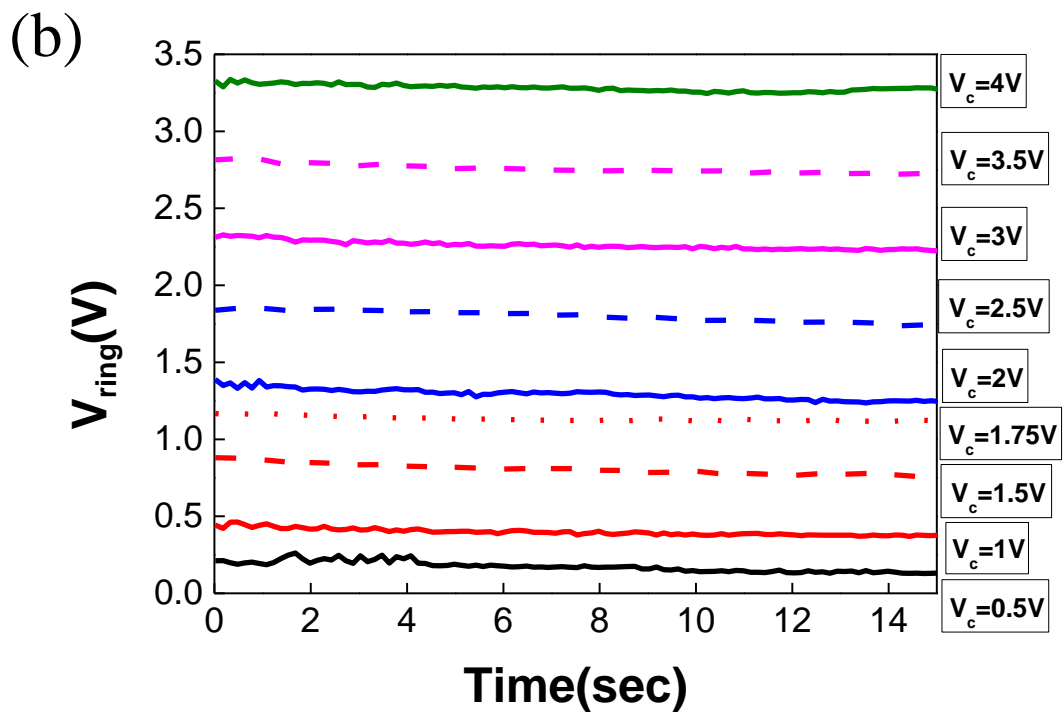
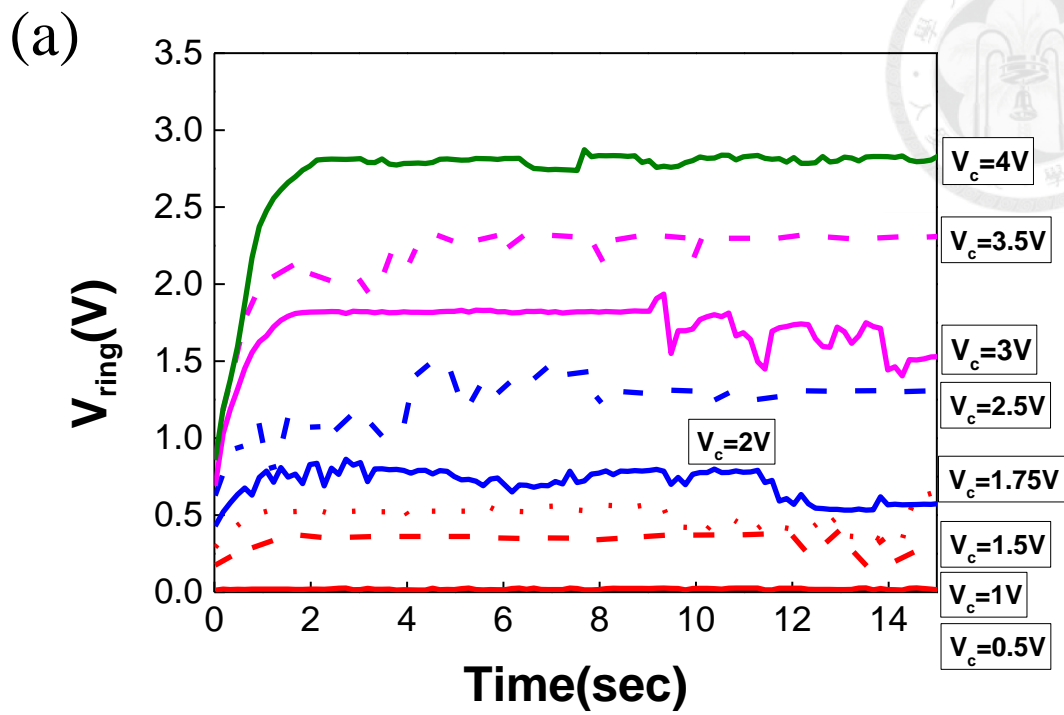
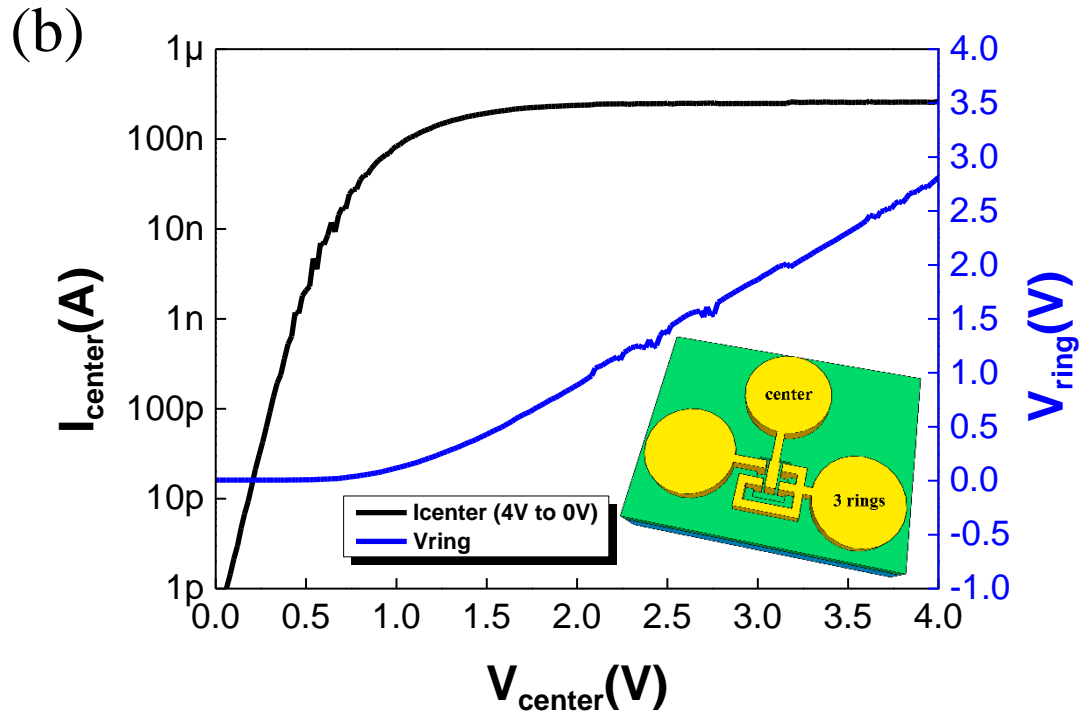
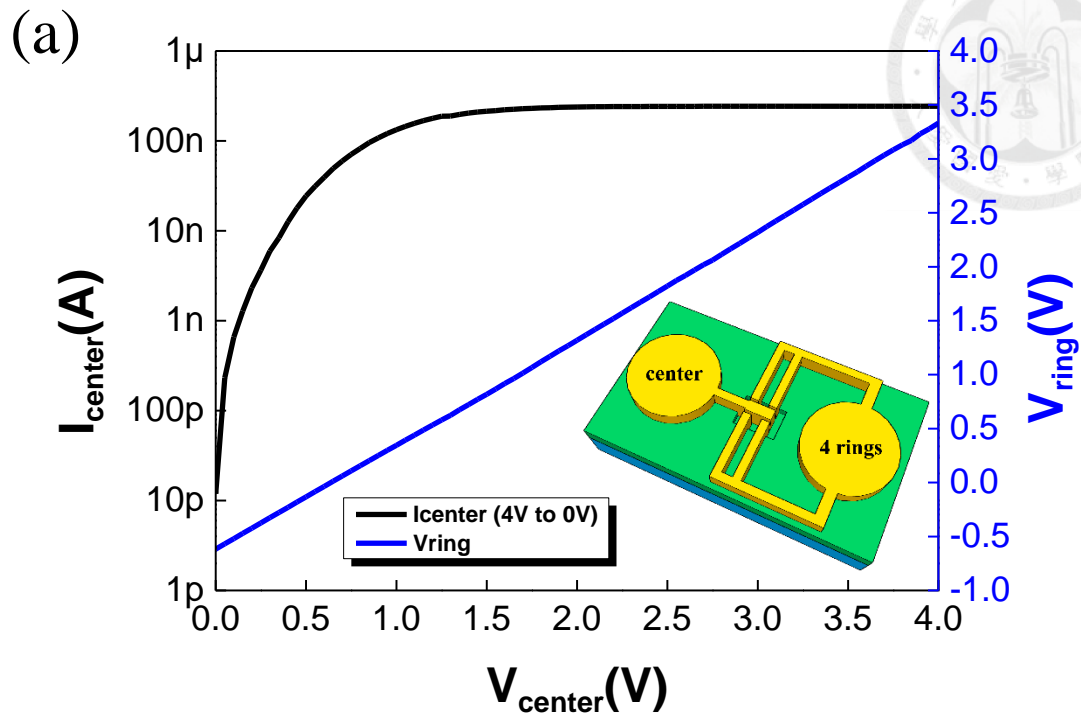
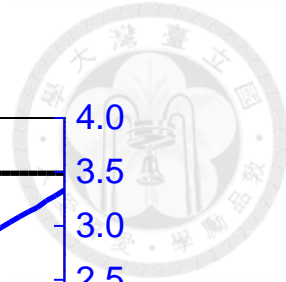


Fig. 3-9. Coupled voltage of  $V_{ring}$  versus time (a) without and (b) with -1 V induced by center during ring soft breakdown operation.



(to be continued)

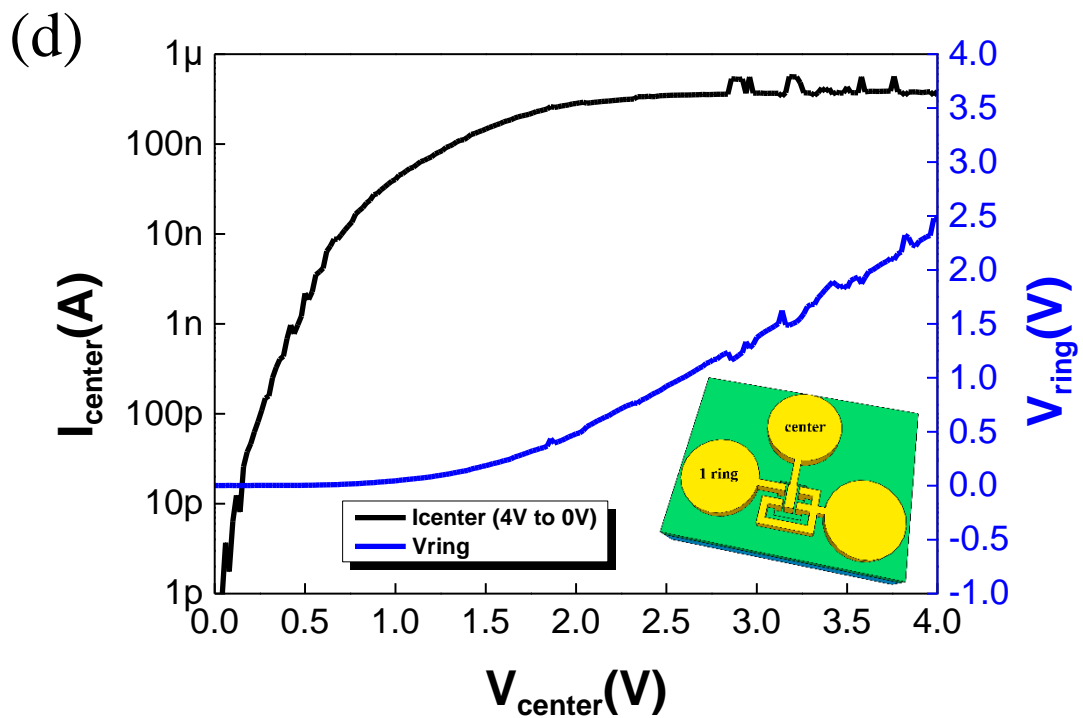
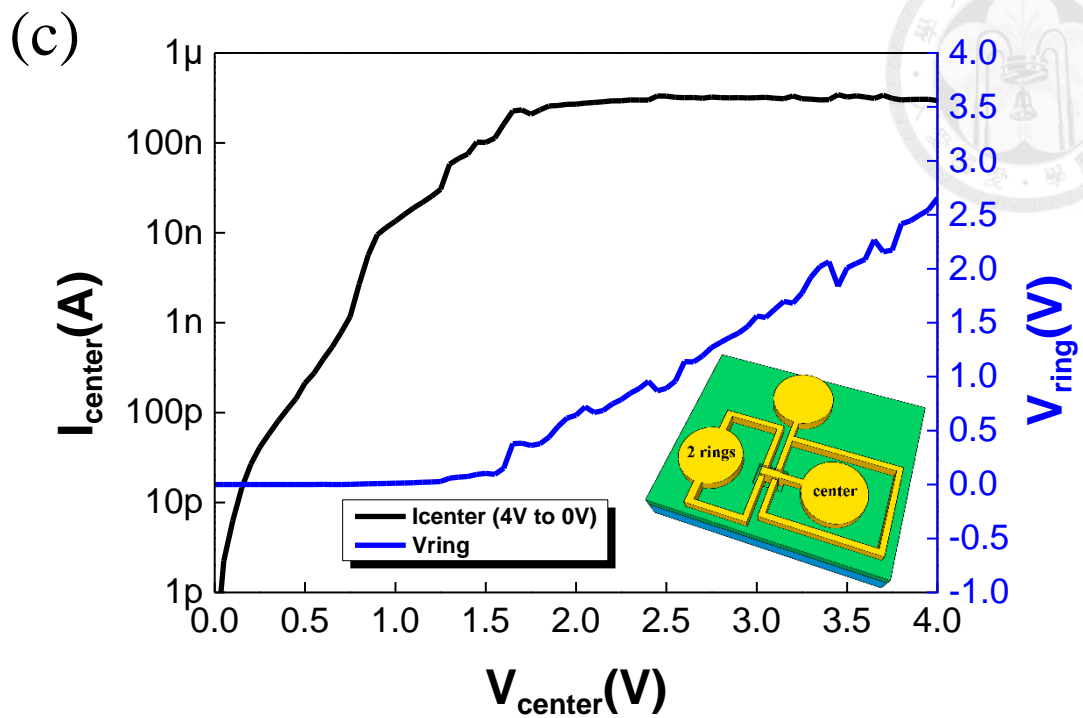


Fig. 3-10.  $I_{\text{center}}$  &  $V_{\text{ring}}$  versus  $V_{\text{center}}$  curves of (a) the 4 rings, (b) the 3 rings, (c) the 2 rings, (d) the 1 ring MIS TD.

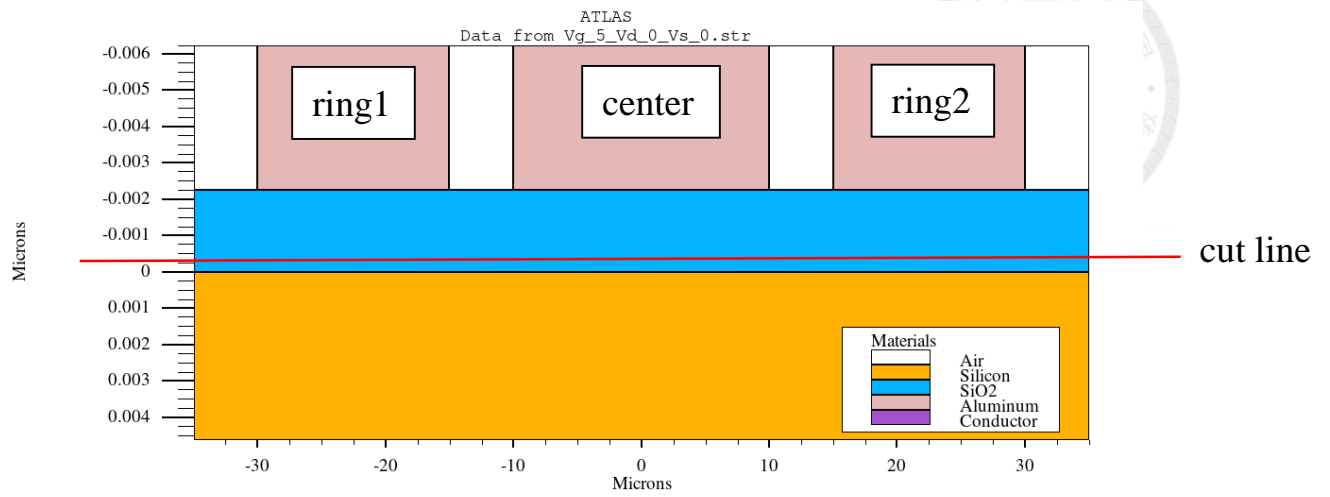


Fig. 3-11. Schematic of the TCAD simulation device for planar oxide.



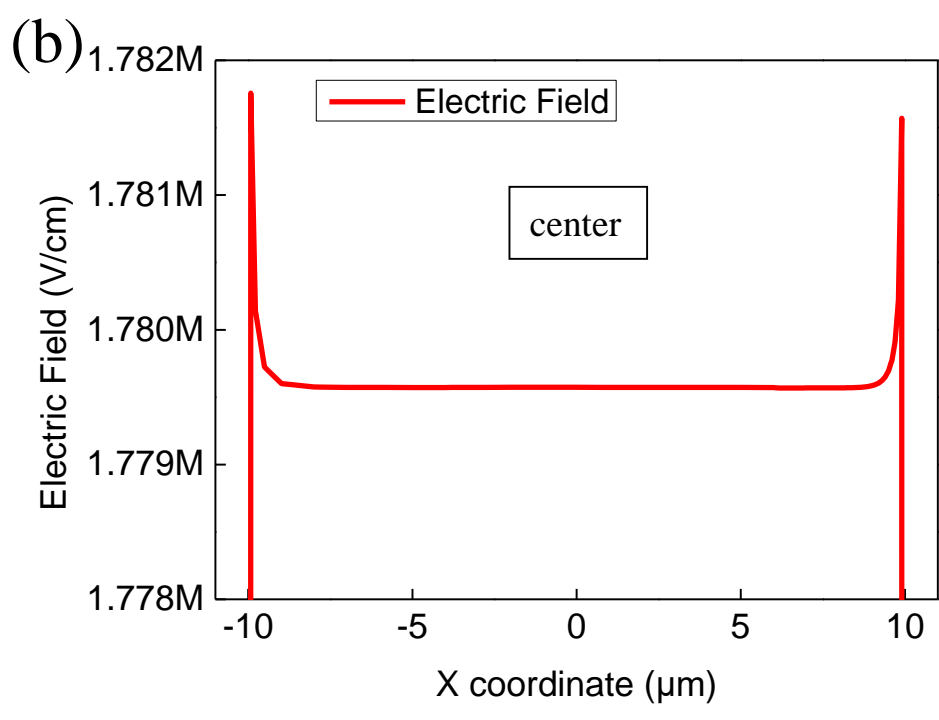
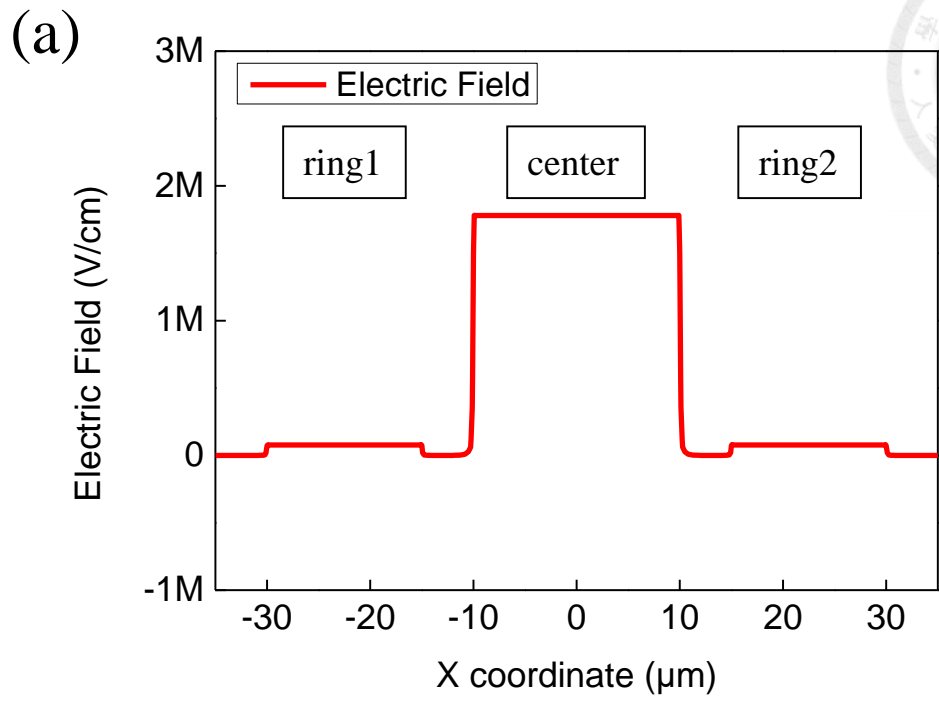


Fig. 3-12. (a) Electric field with  $V_{\text{ring1}} = V_{\text{ring2}} = 0$  V,  $V_c = 5$  V for planar oxide. (b) Zoom in electric field of (a).

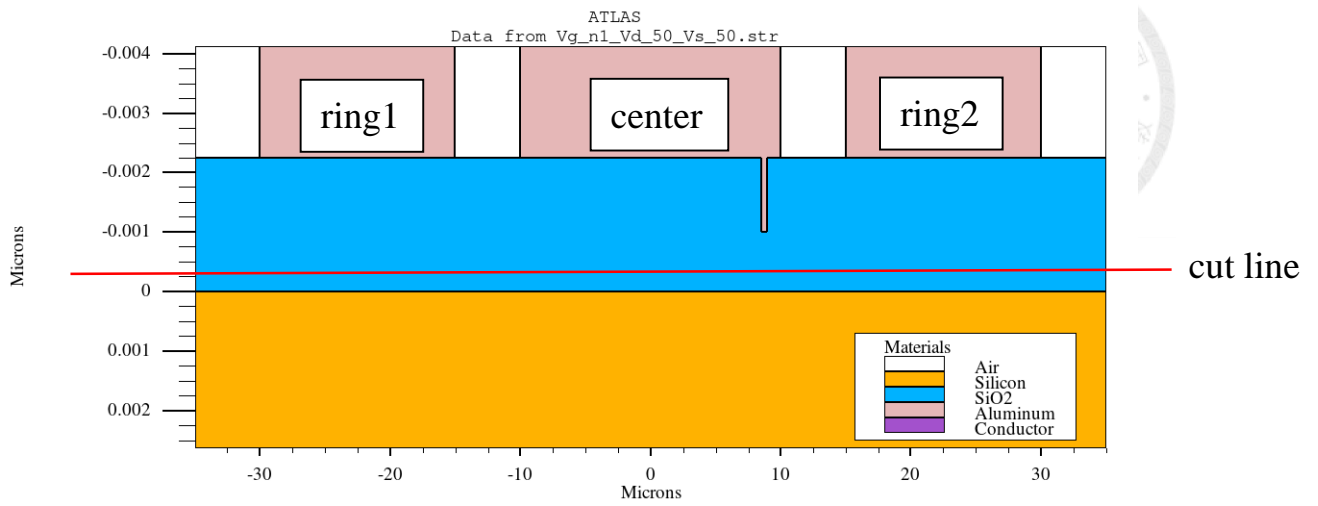
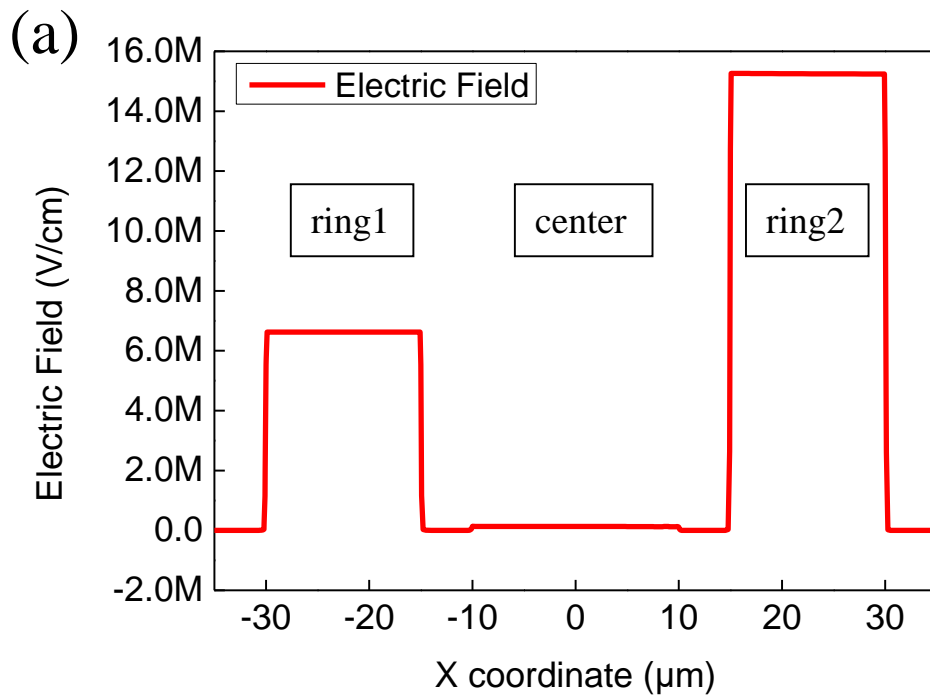


Fig. 3-13. Schematic of the TCAD simulation device with OLT at the edge of center oxide.



(to be continued)

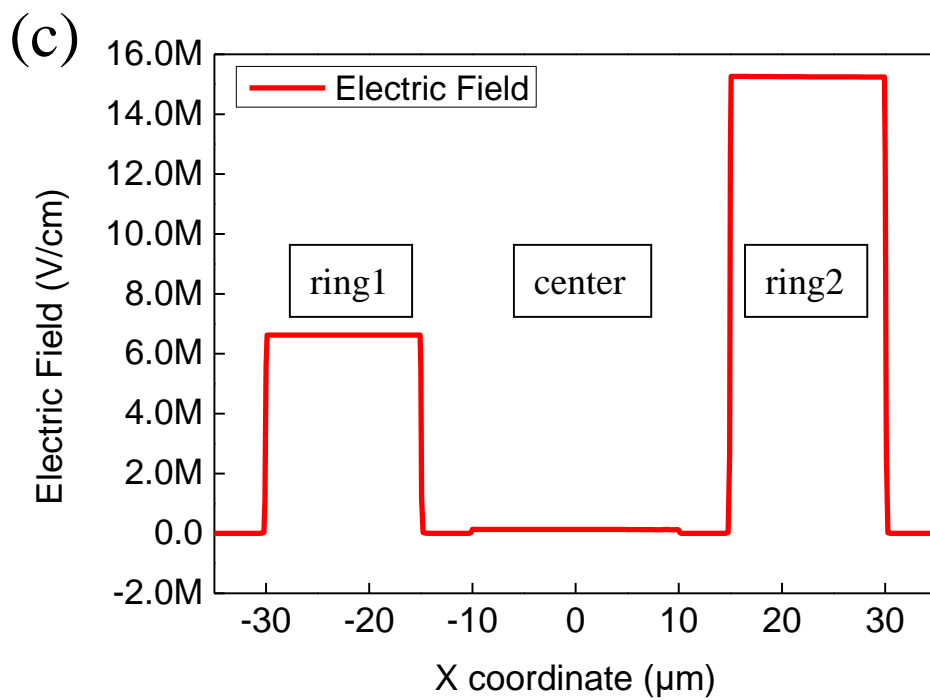
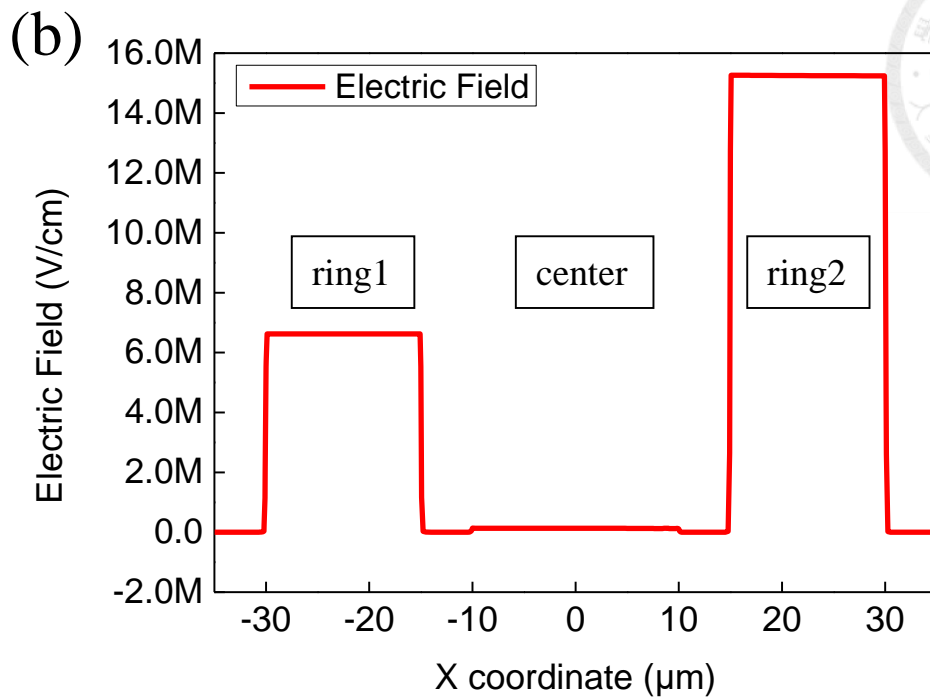


Fig. 3-14. Electric field distributions with (a)  $V_{\text{ring1}} = V_{\text{ring2}} = 3 \text{ V} / V_c = -1 \text{ V}$ , (b) with

$V_{\text{ring1}} = V_{\text{ring2}} = 4 \text{ V} / V_c = -1 \text{ V}$ , and (c) with  $V_{\text{ring1}} = V_{\text{ring2}} = 5 \text{ V} / V_c = -1 \text{ V}$ , for device

with OLT at the edge of center oxide.

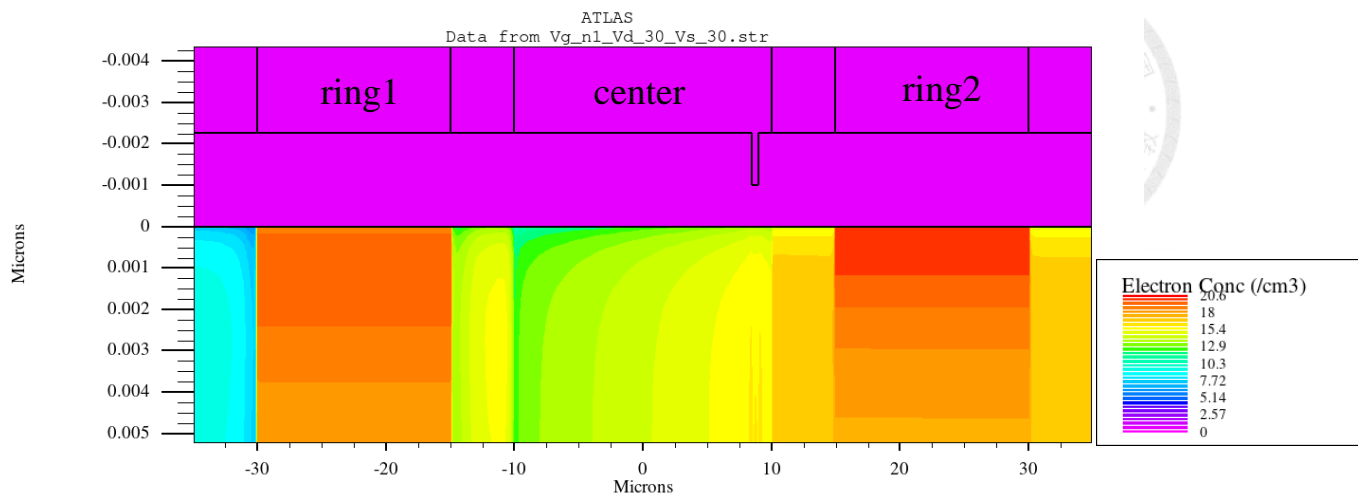


Fig. 3-15. Electron concentration distribution with  $V_{\text{ring1}} = V_{\text{ring2}} = 3 \text{ V} / V_c = -1 \text{ V}$  of the device with OLT at the edge of center oxide.

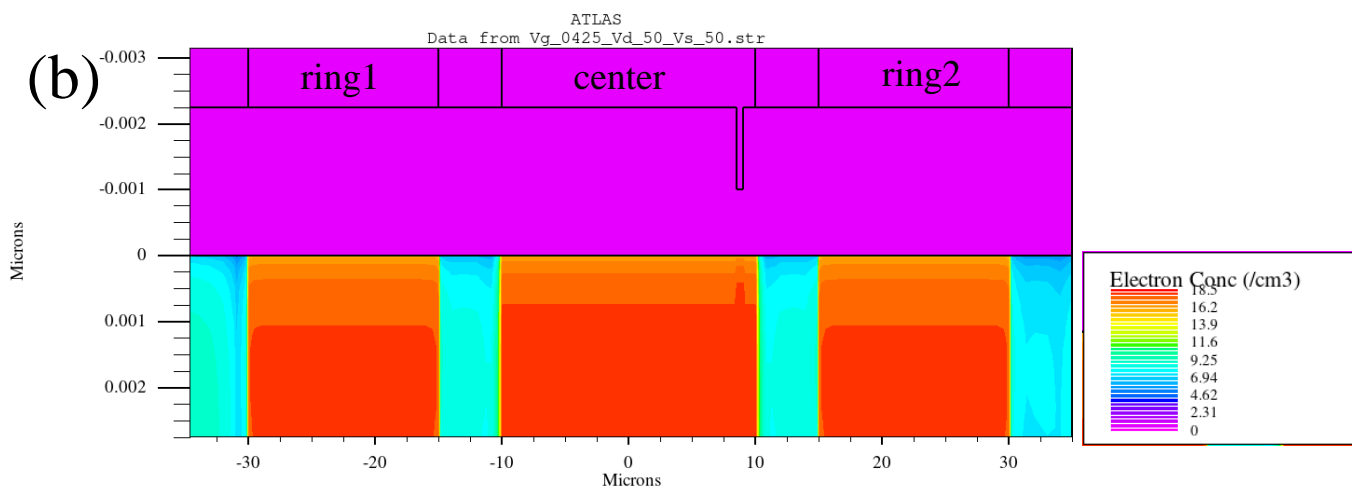
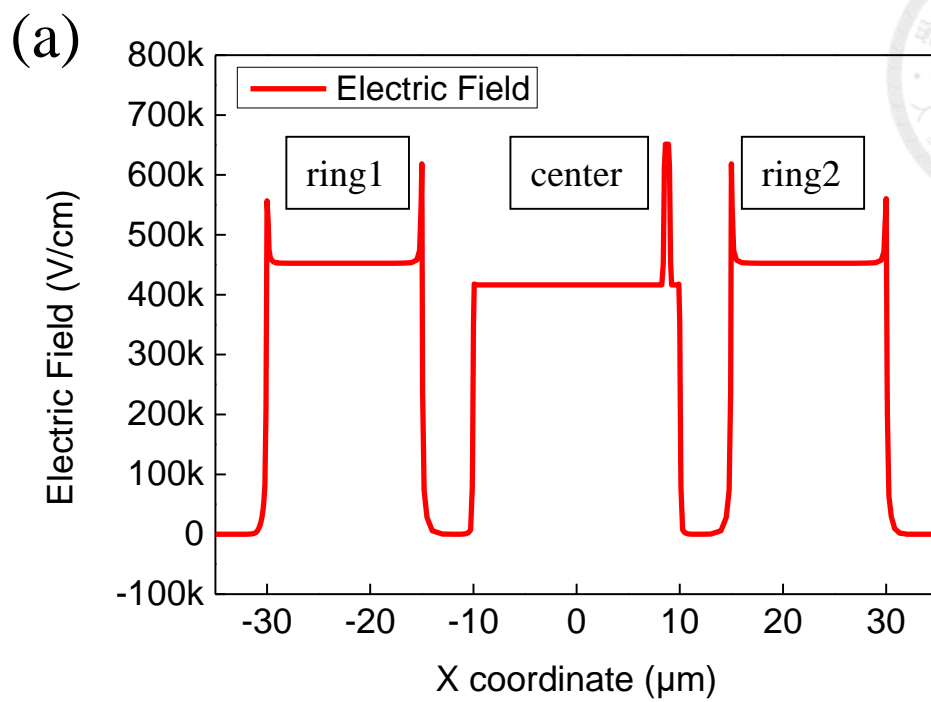


Fig. 3-16. (a) Electric field and (b) Electron concentration with  $V_{\text{ring1}} = V_{\text{ring2}} = 5 \text{ V}$  for center floating condition. The center set voltage is  $V_{\text{set}@I=0} = V_{\text{oc(coupled)}} = 0.425 \text{ V}$ .

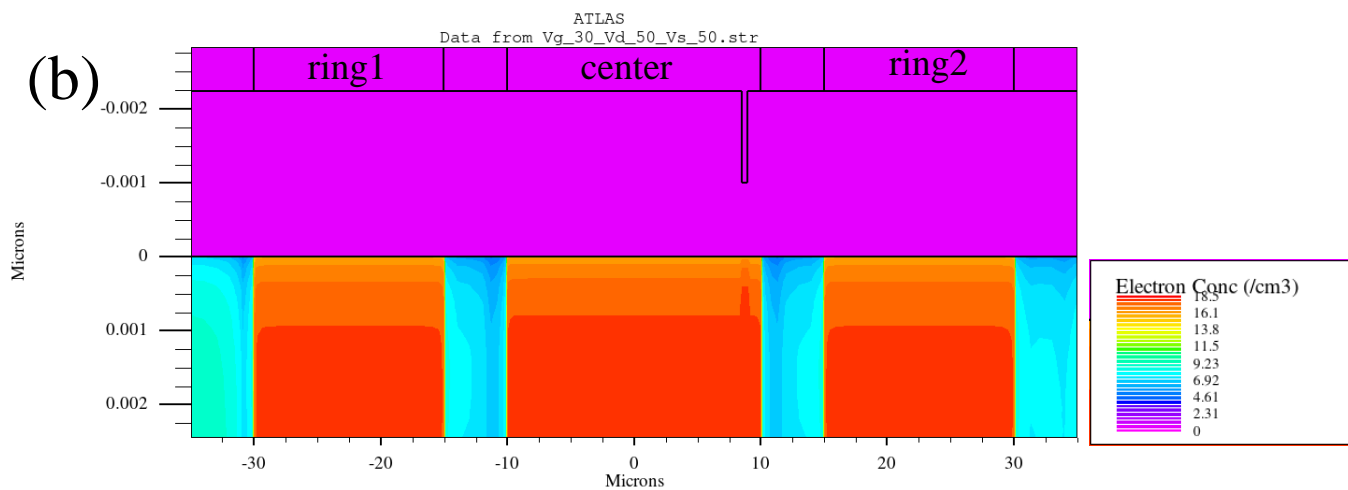
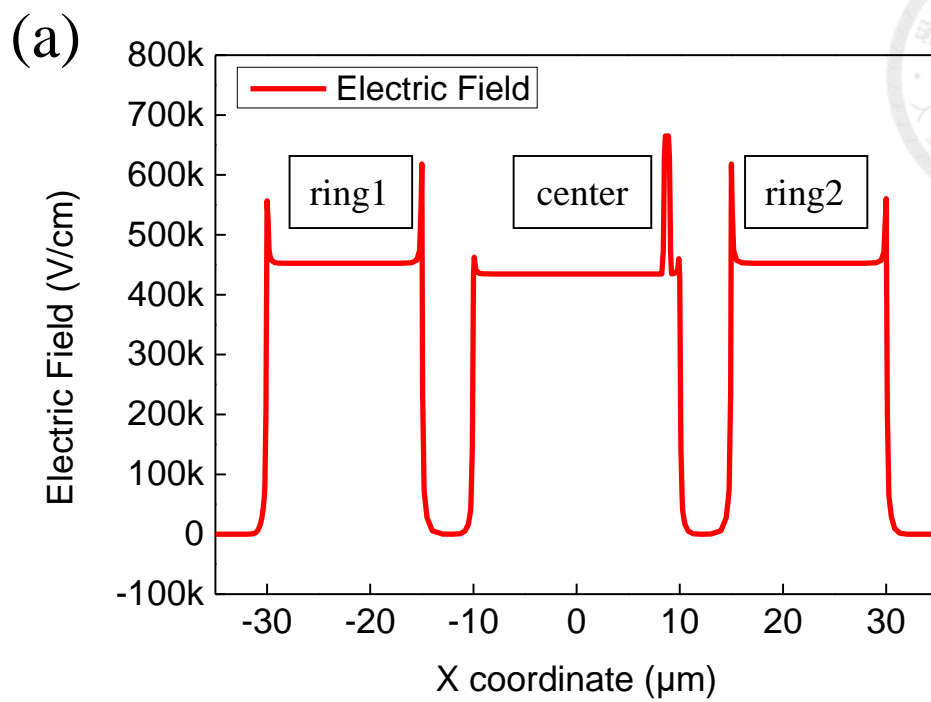


Fig. 3-17. (a) Electric field and (b) Electron concentration with  $V_{\text{ring1}} = V_{\text{ring2}} = 5 \text{ V}$  /

with center bias voltage of  $V_c = 3 \text{ V}$ .





# **Chapter 4**

## **Conclusion and Future Work**

### **4-1 Conclusion**

### **4-2 Future Work**

#### **4-2-1 More Input and Output Combinations for Multi-State**


##### **Characteristic**

#### **4-2-2 Process for High-Low Structure**

#### **4-2-3 The Pattern of Electrode**



## 4-1 Conclusion



After the discussion in the first three chapters, it can be known that the MIS(p) TD with the ultra-thin oxide layer will have a low saturation current under the reverse bias. By designing the pattern of electrode, it can be designed as coupling devices. Because the saturation current is extremely low, the devices can achieve the purpose of low power consumption. The coupling devices are mainly composed of 4 rings and 1 center in this work. Applying a bias voltage to the ring can be used as an input, and the center can be used as a sensor to sense open-circuit voltage or short-circuit current. The sensed open-circuit voltage and short-circuit current can display the multi-state characteristic. Further, the devices are scaled down to meet the current technology nodes. The center and the rings are located in the thin oxide region by using the high-low process. Because the thick oxide region will provide extra minority carriers to the thin oxide region, the current will not be saturated under the reverse bias. Hence, the devices will have no coupling effect. The soft breakdown operation can generate OLT, and the characteristics of the devices are changed to have coupling effect. A method of induced soft breakdown is proposed. The special method through current compliance and the electric field induced by negative bias, one can improve the coupling performance of the devices. Further, the TCAD simulation is also used to prove and explain the distribution of the electric field and

electron concentration of the induced soft breakdown operation.



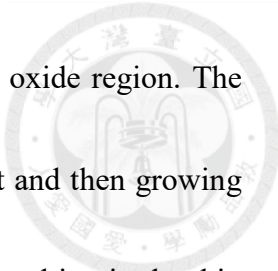
## **4-2 Future Work**

### **4-2-1 More Input and Output Combinations for Multi-State Characteristic**

Originally, there are two points to measure. One point is used as input and one point is used as output. In order to perform better multi-state characteristic, it can be increased to three points to measure. Two points are used as input, and one point is used as output. That is, two rings can be applied with bias voltage at the same time and the applied bias can have different combinations, such as 1 V / 1 V, 2 V / 1 V, 3 V / 2 V. It is believed that the sensed open-circuit voltage and the sensed short-circuit current of the center can exhibit more multilevel characteristic. On the other hand, one point is used as input, and two points are used as output. For example, a bias voltage is applied to the center, and the sensed open-circuit voltage and sensed short-circuit current were read on the two rings. Consequently, if the number of rings is increased, there will be more combinations.

### **4-2-2 Process for High-Low Structure**

In this work, the high-low structure process was done by growing thick oxide first and then thin oxide. On the whole wafer, the area occupied by the thin oxide is extremely small. The quality of the thin oxide region is critical to the electrical characteristics,

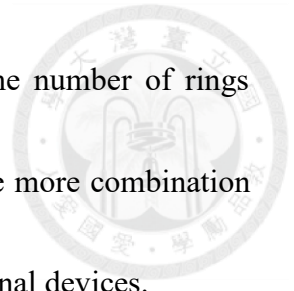


because the center and the ring of the device are located in the thin oxide region. The thick oxide region is just for measurement. Growing thick oxide first and then growing thin oxide may make the interface of the thin oxide region uneven, resulting in the thin oxide region not being exactly planar. The junction of the thick oxygen region and the thin oxygen region may also have a non-ideal contact surface. The thick oxide region will affect the electric field distribution of ANO process, so the thickness of the thin oxide region is difficult to control. Therefore, the process of growing thin oxide first and then thick oxide can be used in the future. The quality of the thin oxide region can be excellent by the process of ANO. By tuning the process time of ANO, the thickness of the thin oxide layer can be effectively controlled. When growing the thick oxide layer, only the thin oxide region needs to be protected by photoresist. Therefore, the planarity of the thin oxide region can be well improved.

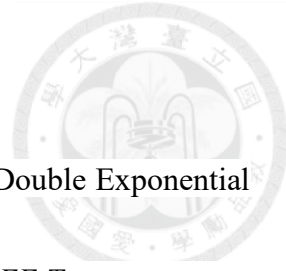
### **4-2-3 The Pattern of Electrode**

The pattern of the electrode is 4 square rings and 1 rectangular center in this work. The pattern of the ring can be changed, such as a rectangle or a circle. Because different patterns may contribute different fringing fields, and the coupling effects will also have different magnitude. In order to achieve more multi-states, the original 4 rings can be increased into more rings, and all the rings can completely surround the center, so that the

coupling effect of the ring to the center can be stronger. When the number of rings increases, it also means that the input increases. Therefore, there are more combination of inputs and outputs, which can show more multilevel than the original devices.



## References

- 
- [1] C. -S. Liao and J. -G. Hwu, "Subthreshold Swing Reduction by Double Exponential Control Mechanism in an MOS Gated-MIS Tunnel Transistor," in *IEEE Transactions on Electron Devices*, vol. 62, no. 6, pp. 2061-2065, June 2015, doi: 10.1109/TED.2015.2424245.
- [2] C. -S. Liao, W. -C. Kao and J. -G. Hwu, "Energy-Saving Write/Read Operation of Memory Cell by Using Separated Storage Device and Remote Reading With an MIS Tunnel Diode Sensor," in *IEEE Journal of the Electron Devices Society*, vol. 4, no. 6, pp. 424-429, Nov. 2016, doi: 10.1109/JEDS.2016.2591956.
- [3] C. -Y. Huang and J. -G. Hwu, "Enhanced Photo Sensing and Lowered Power Consumption in Concentric MIS Devices by Monitoring Outer Ring Open-Circuit Voltage With Biased Inner Gate," in *IEEE Transactions on Electron Devices*, vol. 68, no. 7, pp. 3417-3423, July 2021, doi: 10.1109/TED.2021.3082813.
- [4] Y. -K. Lin and J. -G. Hwu, "Photosensing by Edge Schottky Barrier Height Modulation Induced by Lateral Diffusion Current in MOS(p) Photodiode," in *IEEE Transactions on Electron Devices*, vol. 61, no. 9, pp. 3217-3222, Sept. 2014, doi: 10.1109/TED.2014.2334704.
- [5] B. Yu, Y. Yuan, H.-P. Chen, J. Ahn, P.C. McIntyre and Y. Taur "Effect and extraction

of series resistance in Al<sub>2</sub>O<sub>3</sub>-InGaAs MOS with bulk-oxide trap,” *Electronics Lett.*, Vol. 49 no. 7, pp. 492-493, Mar. 2013.

[6] Kao, Wei-Chih, Jun-Yao Chen, and Jenn-Gwo Hwu. "Transconductance sensitivity enhancement in gated-MIS (p) tunnel diode by self-protective effective local thinning mechanism." *Applied Physics Letters* 109.6 (2016): 063503.

[7] S. -W. Huang and J. -G. Hwu, "Improved Two States Characteristics in MIS Tunnel Diodes by Oxide Local Thinning Enhanced Transient Current Behavior," in *IEEE Transactions on Electron Devices*, vol. 69, no. 12, pp. 7107-7112, Dec. 2022, doi: 10.1109/TED.2022.3215103.

[8] C. C. Lin, P. L. Hsu, L. Lin and J. G. Hwu, “Investigation on Edge Fringing Effect and Oxide Thickness Dependence of Inversion Current in MOS Tunneling Diodes with Comb-Shaped Electrodes,” *J. Appl. Phys.*, vol. 115, no. 12, pp. 124109, Mar. 2014.

[9] C. -Y. Yang and J. -G. Hwu, "Photo-Sensitivity Enhancement of HfO<sub>2</sub>-Based MOS Photodiode With Specific Perimeter Dependency Due to Edge Fringing Field Effect," in *IEEE Sensors Journal*, vol. 12, no. 6, pp. 2313-2319, June 2012, doi: 10.1109/JSEN.2012.2187886.

[10] Chen, Jen-Hao, Kung-Chu Chen, and Jenn-Gwo Hwu. "Fringing field induced current coupling in concentric metal–insulator–semiconductor (MIS) tunnel diodes with

ultra-thin oxide." AIP Advances 12.4 (2022): 045116.

[11] P. F. Schmidt, and W. Michael, "Anodic Formation of Oxide Films on Silicon," J.

Electrochem. Soc., vol. 104, no. 4, pp. 230-236, Apr. 19



